COMPRESSIVE STRENGTH OF SANDSTONE UNDER TRUE TRIAXIAL STRESS STATES

Chaowarin Walsri

A Thesis Submitted in Partial Fulfillment of the Requirements for the

Degree of Master of Engineering in Geotechnology

Suranaree University of Technology

Academic Year 2009

ค่ากำลังแรงกดของหินทรายภายใต้ความเค้นในสามแกนจริง

นายเชาวริน วัลย์ศรี

วิทยานิพนธ์นี้เป็นส่วนหนึ่งของการศึกษาตามหลักสูตรปริญญาวิศวกรรมศาสตรมหาบัณฑิต
สาขาวิชาเทคโนโลยีธรณี
มหาวิทยาลัยเทคโนโลยีสุรนารี
ปีการศึกษา 2552

COMPRESSIVE STRENGTH OF SANDSTONE UNDER TRUE TRIAXIAL STRESS STRATES

Suranaree University of Technology has approved this thesis submitted in partial fulfillment of the requirements for the Master's degree.

Thesis Examining Committee

_____

(Asst. Prof. Thara Lekuthai)

Chairperson

_____

(Assoc. Prof. Dr. Kittitep Fuenkajorn)

Member (Thesis Advisor)

_____

(Dr. Prachaya Tepnarong)

Member

_____

(Prof. Dr. Pairote Sattayatham)

Acting Vice Rector for Academic Affairs

_____

(Assoc. Prof. Dr. Vorapot Khompis)

Dean of Institute of Engineering

เชาวริน วัลย์ศรี : ค่ากำลังแรงกดของหินทรายภายใต้ความเค้นในสามแกนจริง (COMPRESSIVE STRENGTH OF SANDSTONE UNDER TRUE TRIAXIAL STRESS STATES) อาจารย์ที่ปรึกษา : รองศาสตราจารย์ ดร.กิตติเทพ เฟื่องขจร, 78 หน้า

วัตถุประสงค์ของการวิจัยนี้คือเพื่อหาค่าความแข็งของหินทรายสามชนิดที่อยู่ในสภาวะความเค้นในสามทิศทางที่ไม่เท่ากันและเพื่อพัฒนาเกณฑ์การวิบัติในสามทิศทางของหินที่สามารถนำมาประยุกต์ใช้ในการออกแบบและวิเคราะห์เสถียรภาพของโครงสร้างทางธรณีวิทยา กิจกรรมหลักประกอบด้วยการทดสอบเพื่อหาความเค้นหลักสูงสุดที่จุดวิบัติของหินภายใต้ความเค้นหลักกลางและค่าความเค้นหลักต่ำสุดในหลายระดับและการพัฒนาความสัมพันทางคณิตศาสตร์ของความเค้นในสามแกนที่จุดวิบัติ ตัวอย่างหินคือหินทรายชุดพระวิหาร ภูพาน และภูกระดึง โดยเตรียมเป็นรูปทรงสี่เหลี่ยม 50x50x100 ลูกบาก์ศมิลลิเมตร เครื่องกดทดสอบในสามแกนจริงจะให้ค่าความเค้นหลักกลางและค่าความเค้นหลักต่ำสุดคงที่ต่อตัวอย่างหินและทำการเพิ่มค่าความเค้นหลักสูงสุดจนถึงจุดวิบัติ ความเค้นหลักกลางและความเค้นหลักต่ำสุดจะมีระดับตั้งแต่ 0 ถึง 15 เมกกะปาสคาล ได้ใช้ตัวอย่างทดสอบอย่างน้อย 20 ตัวอย่างต่อหินทรายหนึ่งชนิดซึ่งขึ้นอยู่กับความสอดคล้องของผลการทดสอบค่าความแข็ง ค่าความเค้นที่จุดวิบัติได้ถูกวัดและรูปแบบของการแตกได้ถูกตรวจสอบ เกณฑ์การแตกในสามทิศทางได้นำเสนอในรูปของค่าความเค้นเฉือนต่อค่าความเค้นเฉลี่ย

ผลของการทดสอบแสดงอย่างชัดเจนว่าค่าความเค้นหลักกลางมีผลกระทบต่อค่าความเค้นหลักสูงสุดที่จุดวิบัติของหินทรายทุกชนิด ผลการทดสอบนี้มีความสอดคล้องกับการทดสอบโดยผู้วิจัยอื่น ภายใต้สภาวะความเค้นในสามแกนจริงนี้เกณฑ์ที่ดัดแปลงจาก Weibols and Cook สามารถคาดคะเนค่าความแข็งของหินทรายที่ได้ทำการทดสอบได้อย่างสมเหตุสมผล เนื่องจากผลกระทบของค่าความเค้นหลักกลางเกณฑ์ของ Coulomb จึงไม่สามารถเป็นตัวแทนค่าความแข็งของหินภายใต้สภาวะแรงกดในสามแกนจริง โดยเฉพาะในสภาวะที่อัตราส่วนระหว่างความเค้นหลักกลางต่อความเค้นหลักต่ำสุดมีค่าสูง ซึ่งคาดว่าผลกระทบของค่าความเค้นหลักกลางเกิดจากการทำงานของกลไกลสองแบบที่มีผลกระทบตรงข้ามกันคือ (1) กลไกจากการแข็งขึ้นของหินในทิศทางตั้งฉากกับระนาบของค่าความเค้นหลักสูงสุดและความเค้นหลักต่ำสุด และ (2) กลไกที่เพิ่มค่าความเครียดดึงในทิศทางของค่าความเค้นหลักสูงสุดและความเค้นหลักต่ำสุด ค่าความเค้น

หลักกลางสามารถทำให้เนื้อหินมีความแข็งขึ้นในระนาบที่ตั้งฉากกับทิศทางของมัน ดังนั้นความแตกต่างของความเค้นจะมีค่าสูงขึ้นที่จุดวิบัติ มีความเชื่อว่าความสัมพันธ์ของขนาดของค่าความเค้นหลักกลางต่อค่าความแข็งของหินอาจไม่เป็นเส้นตรง โดยเฉพาะในกรณีที่มีค่าความเค้นหลักกลางสูง ความสัมพันธ์จะขึ้นอยู่กับชนิดของหินและเนื้อหินของมันเอง (เช่น การกระจายตัวของขนาดของเม็ดหิน ช่องว่าง รอยแตกและรอยร้าว และชนิดของแร่ประกอบหิน)

สาขาวิชา เทคโนโลยีธรณี ลายมือชื่อนักศึกษา _____

ปีการศึกษา 2552 ลายมือชื่ออาจารย์ที่ปรึกษา _____

CHAOWARIN WALSRI : COMPRESSIVE STRENGTH OF SANDSTONE UNDER TRUE TRIAXIAL STRESS STATES. THESIS ADVISOR : ASSOC. PROF. KITTITEP FUENKAJORN, Ph.D., PE., 78 PP.

ROCK/TRUE TRIAXIAL LOAD FRAM/ INTERMEDIATE PRINCIPLE STRESS/ MAXIMUM PRINCIPAL STRESS

The objectives of this research are to determine the compressive strengths of three types of sandstone subjected to polyaxial stress states, and to develop a three-dimensional failure criterion of the rocks that can be readily applied in the design and stability analysis of geologic structures. The efforts involve determination of the maximum principal stress at failure of the sandstone samples under various intermediate and minimum principal stresses, and development of a mathematical relationship between the three stresses at failure. The sandstone samples belong to the Phra Wihan, Phu Phan, and Phu Kradung formations. They are prepared to obtain 50x50x100 square mm. A polyaxial loading frame is used to apply constant σ_2 and σ_3 onto the specimen while the σ_1 is increased until failure. The applied σ_2 and σ_3 at different magnitudes are varied from 0 to 15 MPa. A minimum of 20 samples are tested for each rock type, depending on the consistency of the strength results. The failure stresses are measured and modes of failure are examined. The three-dimensional strength criterion is derived by presenting the octahedral shear strength as a function of the octahedral mean stress.

The strength results clearly show that σ_2 affects the maximum stress, σ_1 at failure for three sandstones. This phenomenon agrees with those observed elsewhere. Under true triaxial compressive stresses the modified Wiebols and Cook criterion can predict the compressive strengths of the tested sandstones reasonably well. Due to the effect of σ_2 the Coulomb criterion can not represent the rock strengths under true triaxial compressions, particularly under high σ_2 to σ_3 ratios. It is postulated that the effects of the intermediate principal stress are caused by two mechanisms working simultaneously but having opposite effects on the rock polyaxial strengths; (1) mechanism that strengthens the rock matrix in the direction normal to σ_1 - σ_3 plane, and (2) mechanism that induces tensile strains in the directions of σ_1 and σ_3. The intermediate principal stress can strengthen the rock matrix on the plane normal to its direction, and hence a higher differential stress is required to induce failure. It is believed that the relationship between σ_2 magnitudes and the degrees of strengthening can be non-linear, particularly under high σ_2. Such relation depends on rock types and their texture (e.g., distribution of grain sizes, pore spaces, fissures and micro-cracks, and types of rock-forming minerals).

School of Geotechnology Student's Signature_____

Academic Year 2009 Advisor's Signature_____

ACKNOWLEDGMENTS

I wish to acknowledge the funding support of Suranaree University of Technology (SUT).

I would like to express my sincere thanks to Assoc. Prof. Dr. Kittitep Fuenkajorn, thesis advisor, who gave a critical review and constant encouragement throughout the course of this research. Further appreciation is extended to Asst. Prof. Thara Lekuthai : Chairman, School of Geotechnology and Dr. Prachya Tepnarong, School of Geotechnology, Suranaree University of Technology who are member of my examination committee. Grateful thanks are given to all staffs of Geomechanics Research Unit, Institute of Engineering who supported my work.

Finally, I most gratefully acknowledge my parents and friends for all their supported throughout the period of this research.

Chaowarin Walsri

TABLE OF CONTENTS

Page

TABLE OF CONTENTS (Continued)

Page

TABLE OF CONTENTS (Continued)

Page

LIST OF TABLES

Table **Page**

LIST OF FIGURES

LIST OF FIGURES (Continued)

Figure **Page**

LIST OF FIGURES (Continued)

Figure **Page**

LIST OF FIGURES (Continued)

Figure **Page**

LIST OF SYMBOLS AND ABBREVIATIONS

A	=	Parameter related to C_0 and μ_i
B	=	parameter related to C_0 and μ_i
C	=	Parameter related to C_0 and μ_i
C_0	=	Uniaxial compressive strength
C_1	=	Parameter related to C_0 and μ_i
E	=	Elastic modulus
J_1	=	The first order of stress invariant
$J_2^{1/2}$	=	The second order of stress invariant
S_o	=	Cohesion
ε_x	=	Horizontal strain
ε_y	=	Vertical strain
ν	=	Poisson's ratio
σ_B	=	Brazilian tensile stress
σ_m	=	Mean stress
σ_n	=	Normal stress
σ_1	=	Maximum principal stress
σ_2	=	Intermediate principal stress
σ_3	=	Minimum principal stress
τ	=	Shear stress
τ_{oct}	=	Octahedral shear stress
ϕ	=	Friction angle

CHAPTER I

INTRODUCTION

1.1 Background and rationale

It has been experimentally found that the intermediate principal stress (σ_2) can notably reduce the maximum principal stress (σ_1) at failure for intact rock specimens. (Haimson, 2006) This suggests that the triaxial compressive strengths obtained from the conventional triaxial compression test (under $\sigma_2 = \sigma_3$), as given by the American Society for Testing and Materials - ASTM, may not truly represent the actual in-situ strength where the rock is subjected to an anisotropic stress state ($\sigma_1 \neq \sigma_2 \neq \sigma_3$). The rock failure criterion derived from such conventional testing therefore may not be conservative. Obtaining rock strengths in the laboratory under an anisotropic stress state is not only difficult but expensive. Special loading device (e.g., polyaxial loading machine or true triaxial load cell) is required. As a result the failure criterion that can take into account the three-dimensional stress states has been extremely rare. Most existing three dimensional failure criteria for brittle rocks are not adequate because they are not in the form that can readily be applied in the actual design and analysis of geological structures.

1.2 Research objectives

The objectives of this research are to determine the compressive strengths of three types of sandstone subjected to anisotropic stress states, and to develop a three-

dimensional failure criterion of the rocks that can be readily applied in the design and stability analysis of geologic structures. The efforts involve determination of the maximum principal stress at failure of the rock samples under various intermediate and minimum principal stresses, and development of a mathematical relationship between the three stresses at failure. A polyaxial loading frame is used to apply constant σ_2 and σ_3 onto the specimen while the σ_1 is increased until failure. The applied σ_2 and σ_3 at different magnitudes are varied from 0 to 15 MPa. The failure stresses will be measured, and mode of failure will be examined. The results will be compared with those obtained from the conventional triaxial compressive strength tests. The three-dimensional strength criterion will be derived by presenting the octahedral shear strength and a function of the octahedral mean stress with correction factors if needed. Such criterion will be useful for determining or predicting the rock strength under anisotropic stress state of the in-situ condition.

1.3 Research methodology

The research methodology shown in Figure 1.1 comprises 5 steps; literature review, sample collection and preparation, laboratory testing, development of mathematical relations and discussions and conclusions.

1.3.1 Literature review

Literature review is carried out to study the previous research on compressive strength in true-triaxial state and effect of intermediate principal stress. The sources of information are from text books, journals, technical reports and conference papers. A summary of the literature review will be given in the thesis.

1.3.2 Sample collection and preparation

Sandstone samples are collected from the site. A minimum of 3 sandstone types are collected. Sample preparation is carried out in the laboratory at the Suranaree University of Technology. Samples prepared for compressive strength test are $5\times5\times10$ cm^3.

1.3.3 Laboratory testing

The laboratory testing includes the conventional and true triaxial compressive strength tests. Both are performed on the three types of sandstone. Their results are used to develop a multi-axial strength criterion.

1.3.4 Development of mathematical relations

Results from laboratory measurements in terms of intermediate principal stresses and strength of rock are used to formulate mathematical relations. Intermediate principal stresses and the applied stresses can be incorporated to the equation, and derive a new failure criterion for rocks under three dimension stress states.

1.3.5 Conclusion and thesis writing

All research activities, methods, and results are documented and complied in the thesis.

1.4 Scope and limitations

The scope and limitations of the research include as follows.

1. Laboratory experiments are conducted on specimens from three types of sandstone from Phu Kradung, Pra Wihan, and Phu Phan formation.

2. The true triaxial testing is made under intermediate principal stress ranging from 0 to 15 MPa.

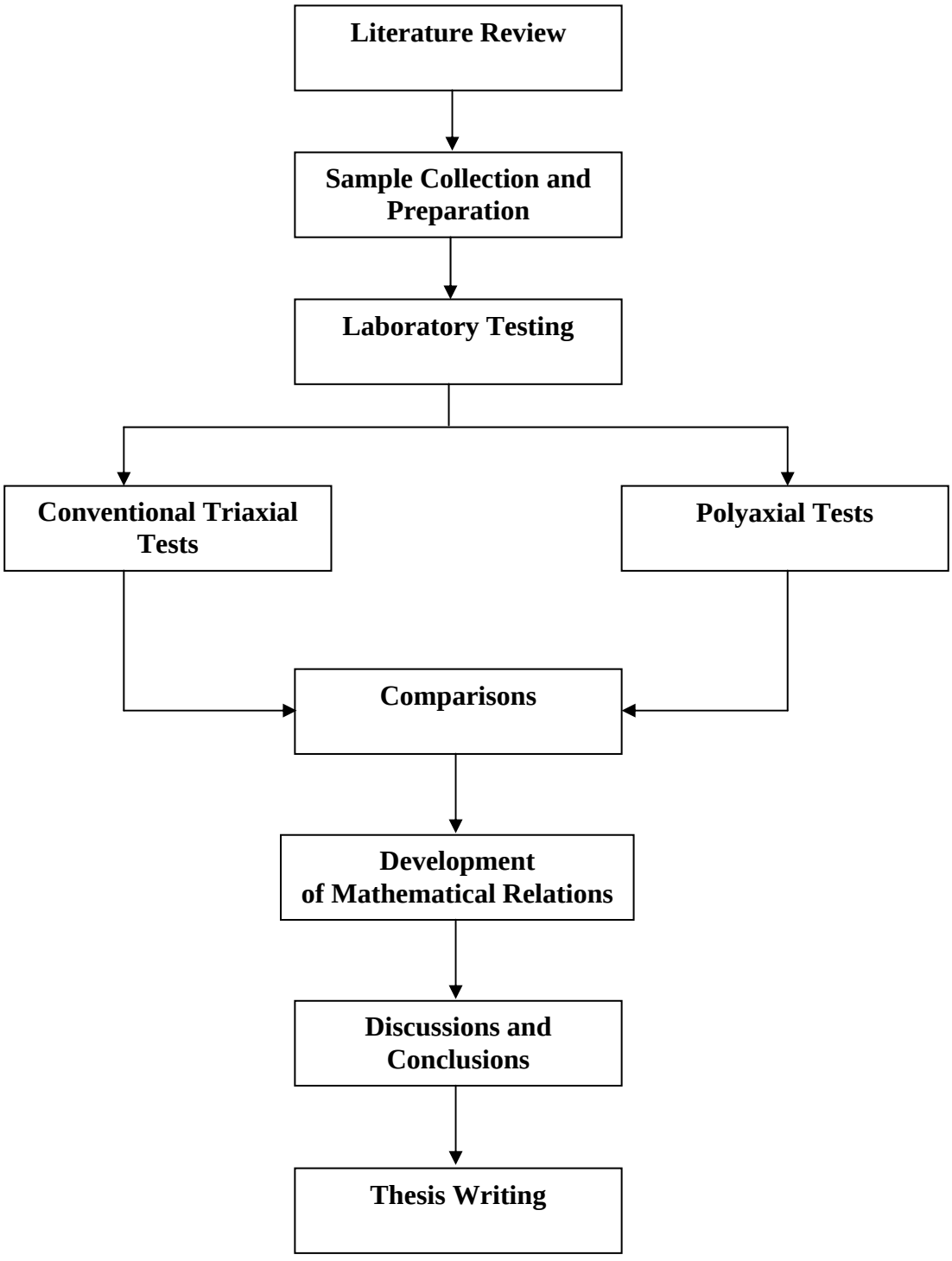

Figure 1.1 Research methodology

3. Up to 20 samples are tested for each rock type, with the nominal sample size of 5×5×10 cm^3

4. All tests are conducted under ambient temperature.

5. Testing is made under dry condition.

6. No field testing is conducted.

1.5 Thesis contents

This research thesis is divided into six chapters. The first chapter includes background and rationale, research objectives, research methodology, and scope and limitations. **Chapter II** presents results of the literature review to improve an understanding of rock compressive strength as affected by the intermediate principal stress. **Chapter III** describes sample collection and preparation. **Chapter IV** describes the laboratory testing; both conventional and true triaxial compressive strength tests. **Chapter V** presents strength criterion. **Chapter VI** is discussions, conclusions and future studies. **Appendix A** provides detailed of technical publications.

CHAPTER II

LITERATURE REVIEW

Relevant topics and previous research results are reviewed to improve an understanding of rock compressive strength as affected by the intermediate principal stress. Summery of the review results is as follows.

Alsayed (2002) used specimens in the form of hollow cylinder specimens for simulating stress condition around the opening to study the behaviour of rock under a much wider variety of stress paths. The hollow cylinder specimens are used in conventional triaxial test cell show in Figure 2.1 It was developed by Hoek and Franklin (1968) and specially designed of internal of pressure loading configuration. Springwell sandstone specimens were subjected to under uniaxial, biaxial, triaxial and polyaxial compression, as well as indirect tension. The results obtained confirm the effect of the intermediate principal stress on rock failure and show that the apparent strength of rock is markedly influenced by the stress condition imposed. Multiaxial testing system can provide realistic prediction of the actual behaviour of rock and guide the formulation of more adequate numerical models.

Kwasniewski et al. (2003) use prismatic samples of medium-grained sandstone from Śląsk Colliery for testing under uniaxial compression, conventional triaxial compression and true triaxial compression conditions. Results of the studies show that confining pressure strongly inhibited dilatant behavior of rock samples tested under conventional triaxial compression conditions; the increasing confinement resulted in the growing compaction of the rock material. The effect of dilatancy was

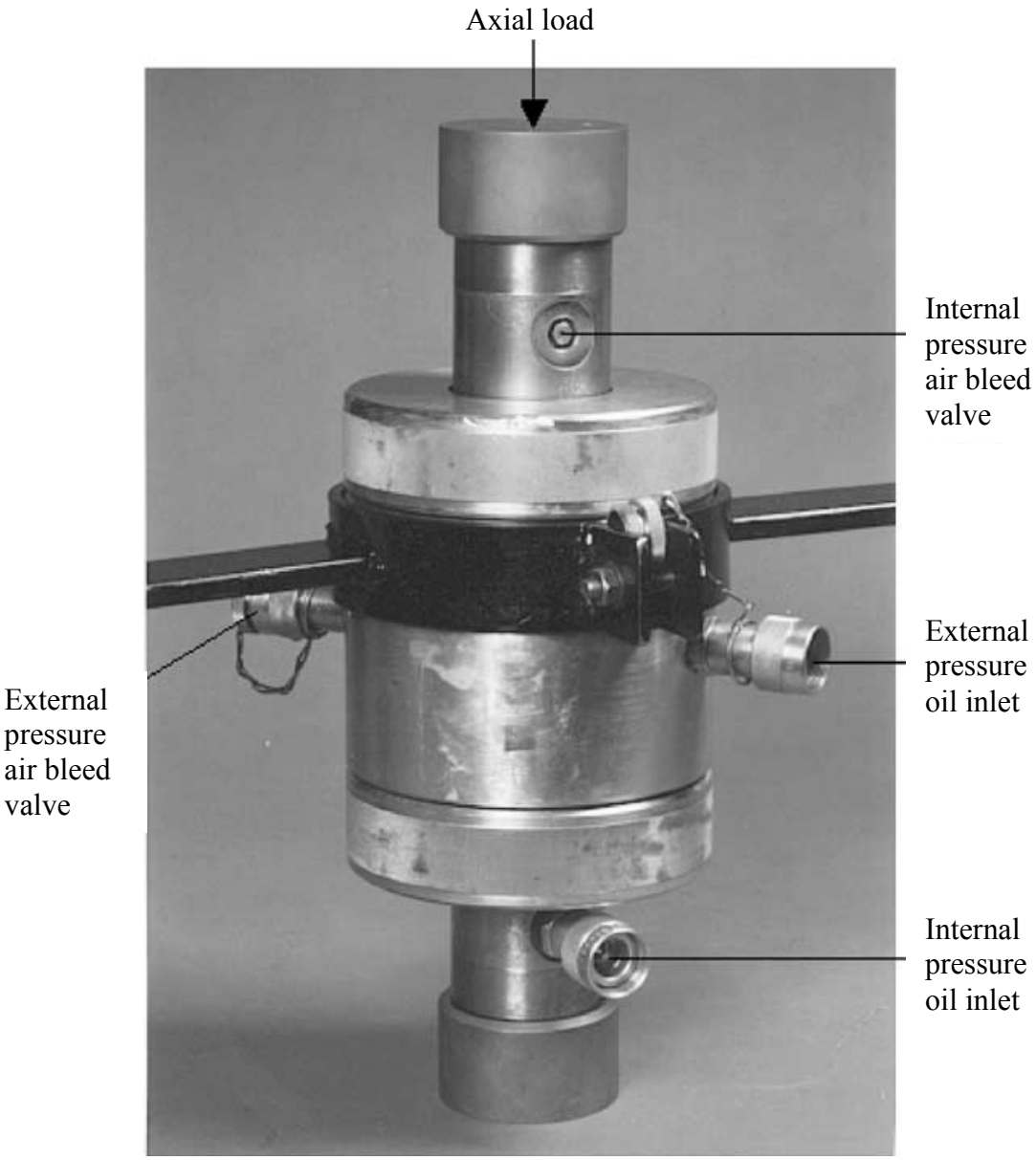

Figure 2.1 Test cell with a specimen inside ready to be transferred to the loading machine (Alsayed, 2002).

also highly suppressed by the intermediate principal stress. While important dilatant, negative volumetric strain corresponded to the peak differential stress at low intermediate principal stress conditions, at high intermediate stresses the rock material was damaged to much lesser extent. As a result, faulting of rock samples

in the post-peak region was much more violent and was accompanied by a strong acoustic effect.

Tiwari and Rao (2004) have described physical modeling of a rock mass under a true triaxial stress state by use block mass models having three smooth joint sets. The testing was using true-triaxial system (TTS) developed by Rao and Tiwari (2002) show in Figure 2.2 The test results show the strength of rock mass (σ_1) and deformation modulus (E_j) increase significantly which is confirmed by fracture shear planes developed on σ_2 face of specimen. Most of the specimens failed in shearing with sliding in some cases. The effect of interlocking and rotation of principal stresses σ_2 and σ_3 on strength and deformation response was also investigated

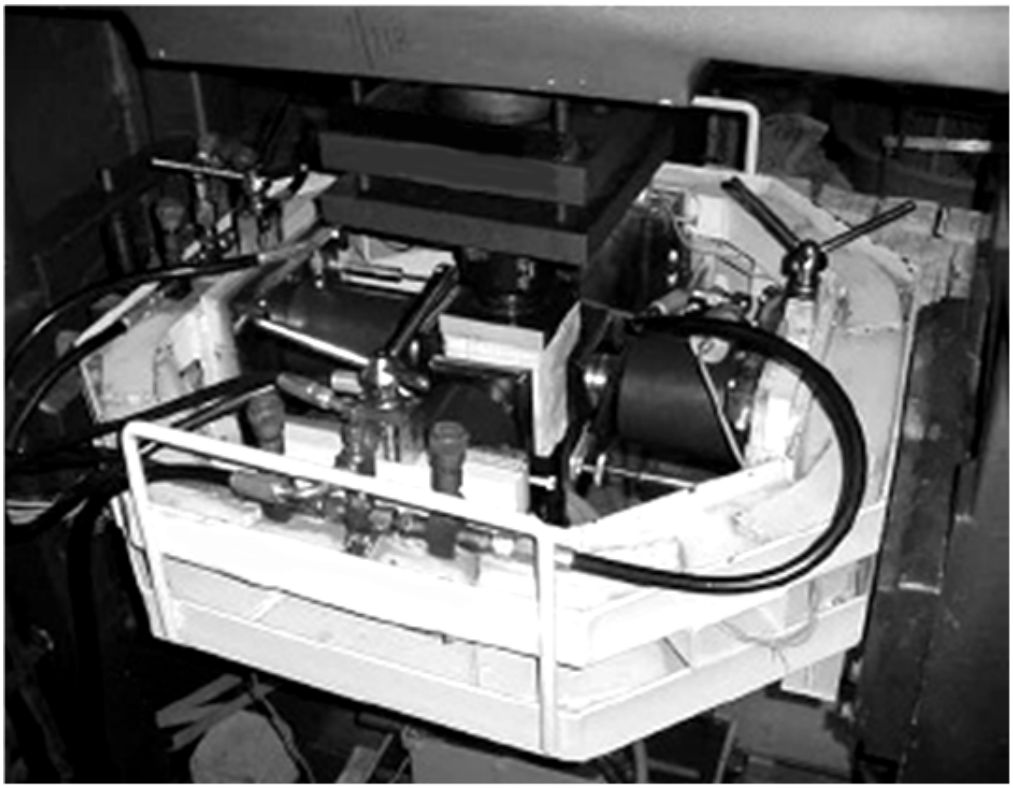

Figure 2.2 True triaxial system used for study (Rao and Tiwari, 2002).

Chang and Haimson (2005) discuss the non-dilatants deformation and failure mechanism under true triaxial compression. They conducted laboratory rock strength experiments on two brittle rocks, hornfels and metapelite, which together are the major constituent of the long valley Caldera (California, USA) basement in the 2025 – 2996 m depth range. Both rocks are banded, very high porosity. Uniaxial compression test at different orientations with respect to banding planes reveal that while the hornfels compressive strength nearly isotropic, the metapelite possesses distinct anisotropy. Conventional triaxial tests in these rocks reveal that their respective strengths in a specific orientation increase approximately linearly with confining pressure. True triaxial compressive experiments in specimens oriented at a consistent angle to banding, in which the magnitude of the least (σ_3) and the intermediate (σ_2) principal stress are different but kept constant during testing while the maximum principal stress is increased until failure, exhibit a behaviour unlike that

previously observed in other rocks under similar testing conditions. For a given magnitude of σ_3, compressive strength σ_1 does not vary significantly in both regardless of the applied σ_2, suggesting little or no intermediate principal stress effect. Strains measured in all three principal directions during loading were used to obtain plots σ_1 versus volumetric strain. Theses are consistently linear almost to the point of rock failure, suggesting no dilatants.

Haimson (2006) describes the effect of the intermediate principal stress (σ_2) on brittle fracture of rocks, and on their strength criteria. Testing equipment emulating Mogi's but considerably more compact was developed at the University of Wisconsin and used for true triaxial testing of some very strong crystalline rocks. Test results revealed three distinct compressive failure mechanisms, depending on loading

mode and rock type: shear faulting resulting from extensile microcrack localization, multiple splitting along the axis, and nondilatant shear failure. The true triaxial strength criterion for the KTB amphibolite derived from such tests was used in conjunction with logged breakout dimensions to estimate the maximum horizontal in situ stress in the KTB ultra deep scientific hole.

Cai (2008) studied the intermediate principal stress on rock fracturing and strength near excavation boundaries using a FEM/ DEM combined numerical tool. A loading condition of $\sigma_3 = 0$ and $\sigma_1 \neq 0$, and $\sigma_2 \neq 0$ exists at the tunnel boundary, where σ_1, σ_2, and σ_3, are the maximum, intermediate, and minimum principal stress components, respectively. The numerical study is based on sample loading testing that follows this type of boundary stress condition. It is seen from the simulation results that the generation of tunnel surface parallel fractures and microcracks is attributed to material heterogeneity and the existence of relatively high intermediate principal stress (σ_2), as well as zero to low minimum principal stress (σ_3) confinement. A high intermediate principal stress confines the rock in such away that microcracks and fractures can only be developed in the direction parallel to σ_1 and σ_2. Stress-induced fracturing and microcracking in this fashion can lead to onion-skin fractures, spalling, and slabbing in shallow ground near the opening and surface parallel microcracks further away from the opening, leading to anisotropic behavior of the rock. Consideration of the effect of the intermediate principal stress on rock behavior should focus on the stress-induced anisotropic strength and deformation behavior of the rocks show in Figure 2.3 It is also found that the intermediate principal stress has limited influence on the peak strength of the rock near the excavation boundary.

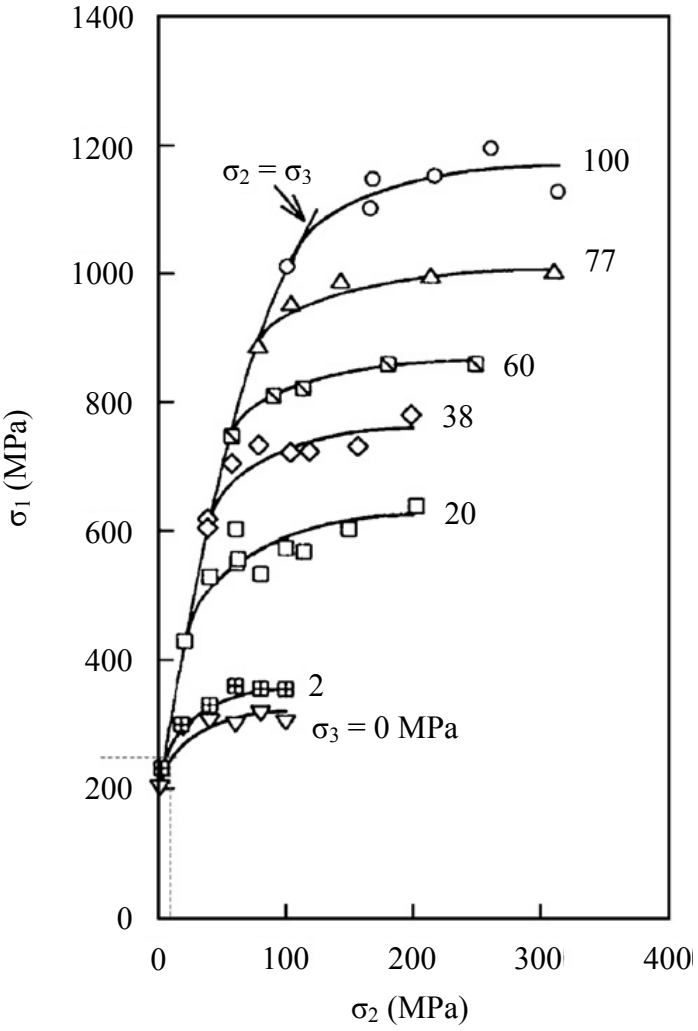

Figure 2.3 Influence of the intermediate principal stress on the strength of Westerly granite. Rapid initial rock strength increases with increasing σ_2 can be seen for low σ_3 (Cai, 2008).

You (2008) reviewed some strength criteria which include the role of the intermediate principal stress, and proposed a new criterion. Strength criteria of the form $\sigma_{oct} = f_n(\sigma_{oct})$, such as Drucker–Prager represent a rotation surface in the principal stress space, symmetric to the line $\sigma_1 = \sigma_2 = \sigma_3$ in the meridian plane. Because $\sigma_{oct} = f_n(\sigma_{oct})$ must fit the pseudo-triaxial compressive strength, it will have a

non-physical outcome for triaxial extension. Mogi's criteria, $\sigma_{oct} = g_1 (\sigma_{m,2})$ and $\sigma_{max} = g_2 (\sigma_b)$ are able to fit experimental data reasonably well, but the prediction of strength is not good and sometimes problematic. Strength criterion with the form $\lambda(\sigma_1, \sigma_2, \sigma_3) = F[\eta(\sigma_1, \sigma_2, \sigma_3)]$, or a curve of two variables which can be decided by fitting pseudo-triaxial experimental data, is not expected to describe the strength under various stress states, no matter how high the correlation coefficient of λ and η is, or how low the misfit of the equation $\lambda = F(\eta)$ is, as these seemingly good correlations usually result from the Dominant influence of the maximum principal stress in the metrics of λ and η. The intermediate principal stress may improve the strength of rock specimen, but its influence will be restricted by σ_3. Also when σ_2 is high enough to cause failure in the $\sigma_2 - \sigma_3$ direction, the strength will decrease with the increasing σ_2. The new strength criterion with exponent form has just such a character, and gives much lower misfits than do all seven criteria discussed by Colmenares and Zoback (2002). A statistical evaluation of intact rock failure criteria constrained by polyaxial test data for five different rocks.

CHAPTER III

SAMPLE PREPARATION

3.1 Introduction

The tested sandstones are from three sources: Phu Phan, Phra Wihan and Phu Kradung formations (hereafter designated as PP, PW and PK sandstones) as shown in Figure 3.1. These fine-grained quartz sandstones are selected primarily because of their highly uniform texture, density and strength. The main mineral compositions of three sandstones obtained from x-ray diffraction analyses are given in Table 3.1. Their average grain size is 0.1-1.0 mm. They are commonly found in the north and northeast of Thailand. Their mechanical properties and responses play a significant role in the stability of tunnels, slope embankments and dam foundations in the region.

3.2 Sample preparation

Sandstone samples are collected from Saraburi province. A minimum of 3 sandstone types are collected. Sample preparation is carried out in the laboratory at the Suranaree University of Technology. Samples prepared for polyaxial compressive strength test are 5×5×10 cm^3 show in Figure 3.2. For the polyaxial compression testing rectangular block specimens are cut and ground to have a nominal dimension of 5×5×10 cm^3. The perpendicularity and parallelism of the specimens follow the ASTM (D 4543-85) specifications. The longest axis is

parallel to the bedding planes and to the direction of the major principal stress. Though having different shape the specimens used here have volume and length-to-diameter ratio comparable to those used in the conventional uniaxial and triaxial compression test methods.

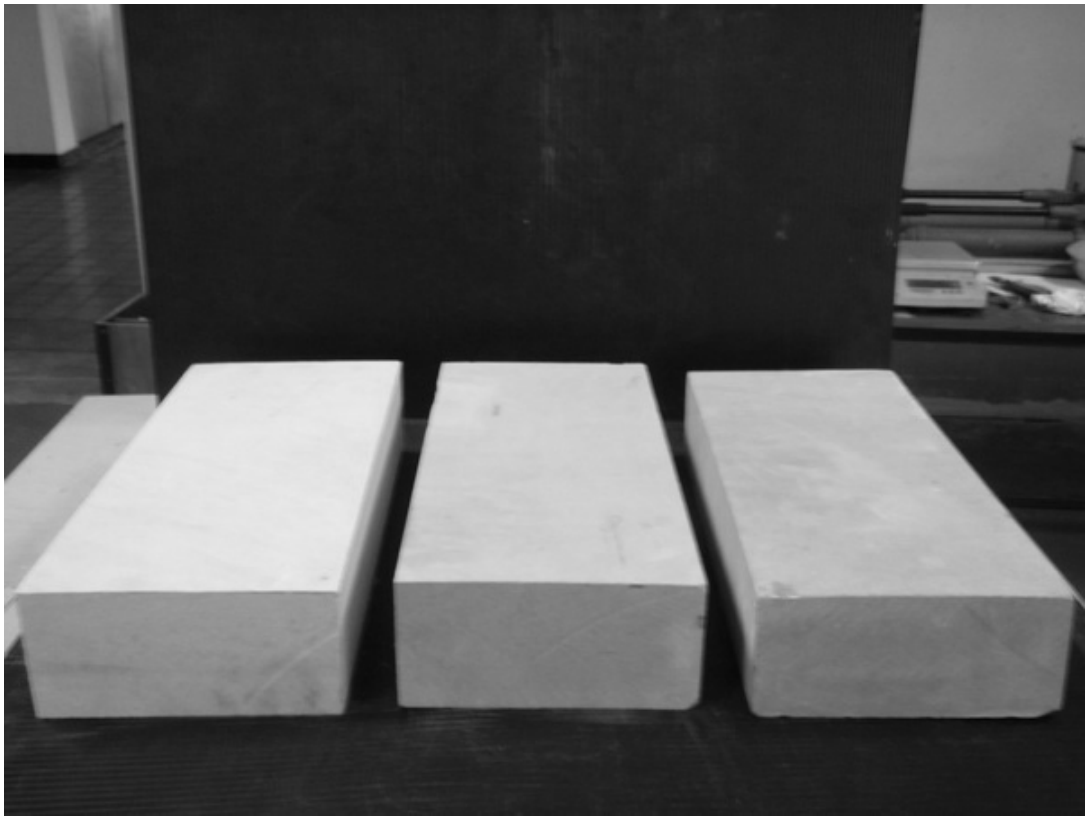

Figure 3.1 Sandstones blocks with nominal size of 10 cm x 20 cm x 40 cm are collected from Saraburi province. Left: Phra Wihan, Middle: Phu Phan and Right: Phu Kadung.

Table 3.1 Mineral composition of three sandstones.

Rock Name	Density (g/cc)	Color	Composition				
			Quartz (%)	Albite (%)	Kaolinite (%)	Feldspar (%)	Mica (%)
PW sandstone	2.35	white	99.47	-	0.53	-	-
PP sandstone	2.45	yellow	98.40	-	-	-	1.60
PK sandstone	2.63	green	48.80	46.10	5.10	-	-

Figure 3.2 Sandstone specimens prepared for true triaxial stress. Left: Phu Kadung, Middle: Phu Phan and Right: Phra Wihan.

CHAPTER IV

LABORATORY EXPERIMENTS

4.1 Introduction

The objectives of this research are to determine the compressive strengths of three types of sandstone subjected to anisotropic stress states, and to develop a three-dimensional failure criterion of the rocks that can be readily applied in the design and stability analysis of geologic structures. This chapter describes the method and results of the laboratory experiments, including characterization tests and polyaxial compressive strength tests.

4.2 Characterization tests

Uniaxial and triaxial compressive strength tests are performed on PW, PP and PK sandstones. The objectives are to develop a data basis to compare with the true triaxial test results.

4.2.1 Uniaxial compressive strength tests (UCS)

Test procedure for the laboratory determination of the UCS strictly follows the American Society for Testing and Materials standard (ASTM D7012-04) and suggested method by ISRM (International Society of Rock Mechanics) (Brown, 1981). Core specimens with a nominal diameter of 54 mm and length-to-diameter ratio of 2.5 are axially loaded to failure (Figure 4.1). The UCS of the specimen is calculated by dividing the maximum load by the original cross-sectional area. Five specimens are tested for each rock type. The results of the uniaxial compressive

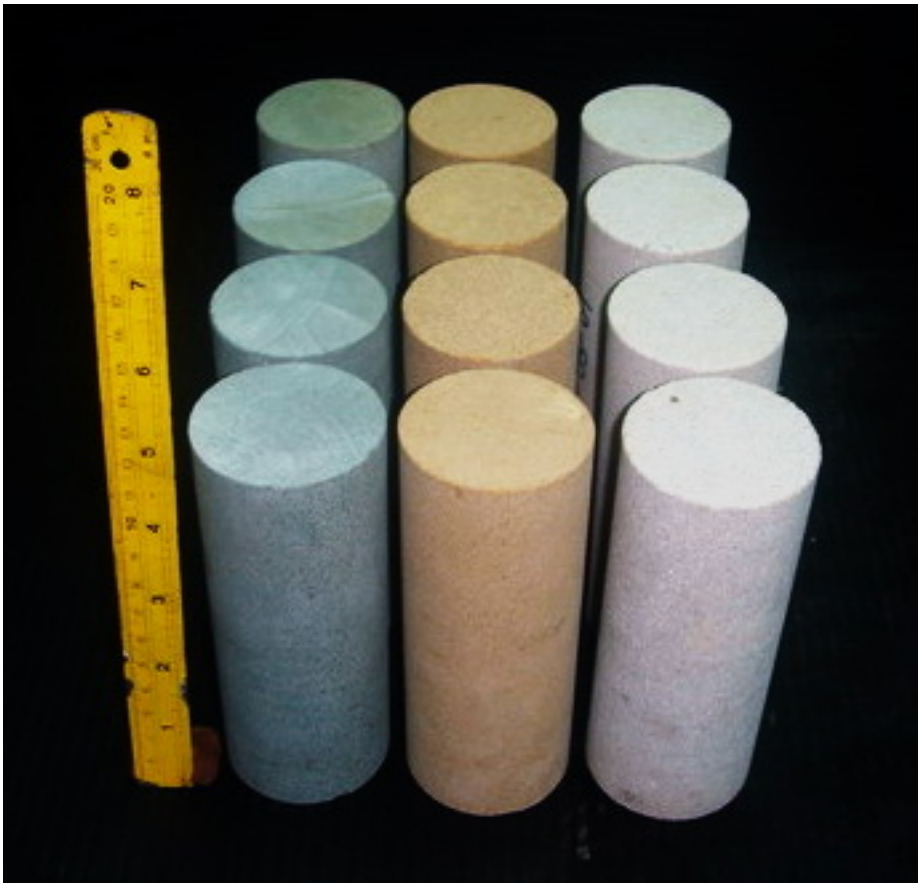

Figure 4.1 PW, PP and PK sandstones specimens prepared for the uniaxial compressive strength test have 54 mm in diameter with L/D ratio of 2.5.

strength test are shown in Table 4.1. Figure 4.2 through 4.4 plots the axial stress as a function of axial strains of PW sandstones.

4.2.2 Triaxial compressive strength tests

The objective of the triaxial compressive strength test is to determine the compressive strength of three sandstones under various confining pressures. The sample preparation and test procedure follow the applicable ASTM standard practice (ASTM D7012-04) and ISRM suggested method (Brown, 1981), as much as practical. The L/D of all specimens equals 2.0. All specimens are loaded to failure under

Table 4.1 Summary of the results from the uniaxial compressive strength testing.

Types	Specimen No.	Length (mm)	Diameter (mm)	Density (g/cc)	Uniaxial Compressive Strength, σ_c (MPa)	Elastic Modulus, E (GPa)
PW	PWSS-01	107.35	53.94	2.39	72.2	9.9
	PWSS-02	105.93	53.92	2.37	72.3	10.0
	PWSS-03	102.71	53.92	2.40	72.3	10.5
	PWSS-04	136.61	53.70	2.39	59.6	9.0
	PWSS-05	136.45	53.63	2.38	57.5	12.0
	Average ± Standard Deviation				**66.8 ± 7.5**	**10.3 ± 1.1**
PP	PPSS-01	105.33	53.71	2.60	79.4	10.1
	PPSS-02	105.35	53.90	2.63	81.1	10.3
	PPSS-03	109.35	53.20	2.63	83.2	11.3
	PPSS-04	135.84	53.65	2.61	81.8	12.0
	PPSS-05	131.32	53.65	2.61	106.1	12.0
	Average ± Standard Deviation				**86.3 ± 11.1**	**11.1 ± 0.9**
PK	PKSS-01	108.17	53.9	2.61	81.1	8.9
	PKSS-02	109.05	53.9	2.62	78.9	8.9
	PKSS-03	108.24	53.22	2.62	81.3	9.9
	PKSS-04	135.64	53.65	2.6	72.9	10.9
	PKSS-05	131.32	53.65	2.63	106.1	12.0
	Average ± Standard Deviation				**84.1 ± 12.7**	**10.1 ± 1.3**

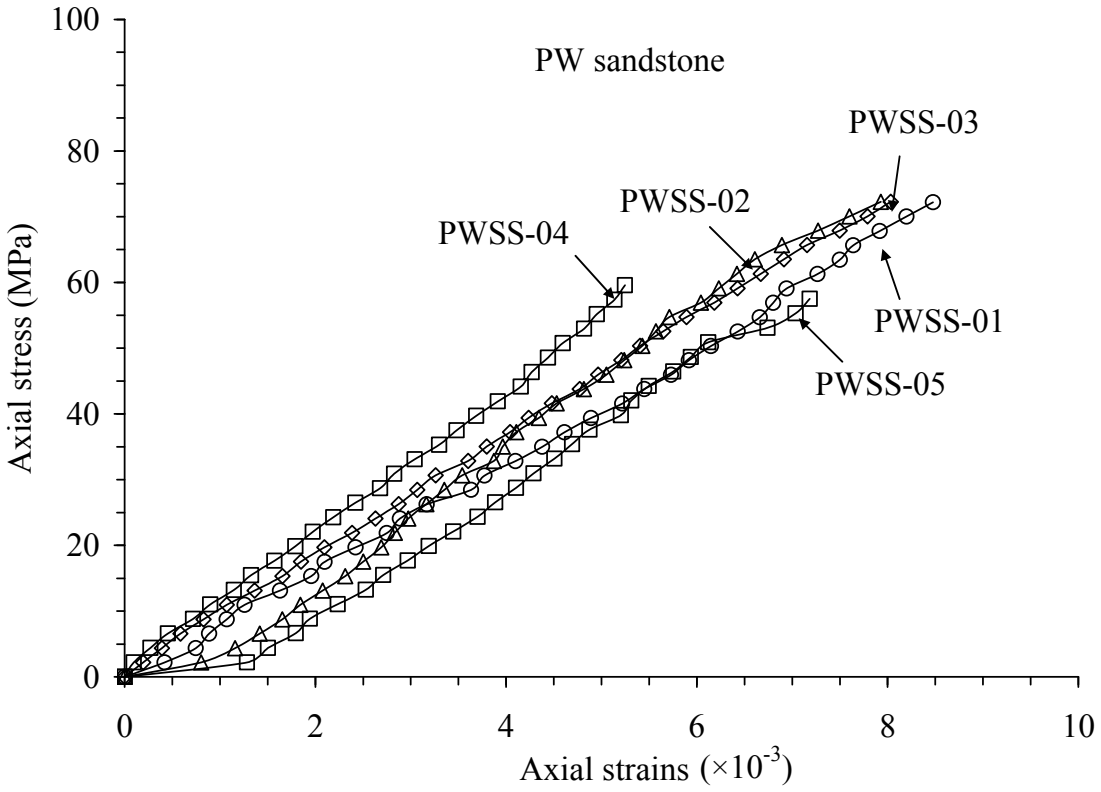

Figure 4.2 Results of uniaxial compressive strength tests of PW sandstone. The axial stresses are plotted as a function of axial strain.

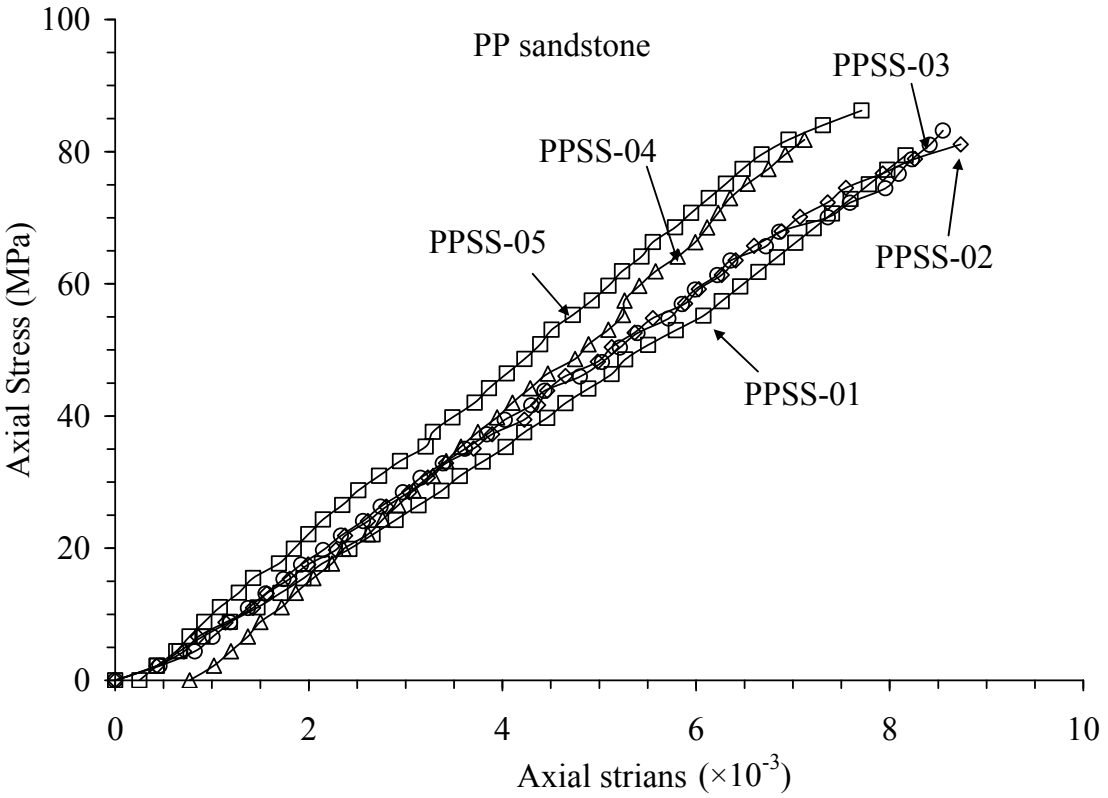

Figure 4.3 Results of uniaxial compressive strength tests of PP sandstone. The axial stresses are plotted as a function of axial strain.

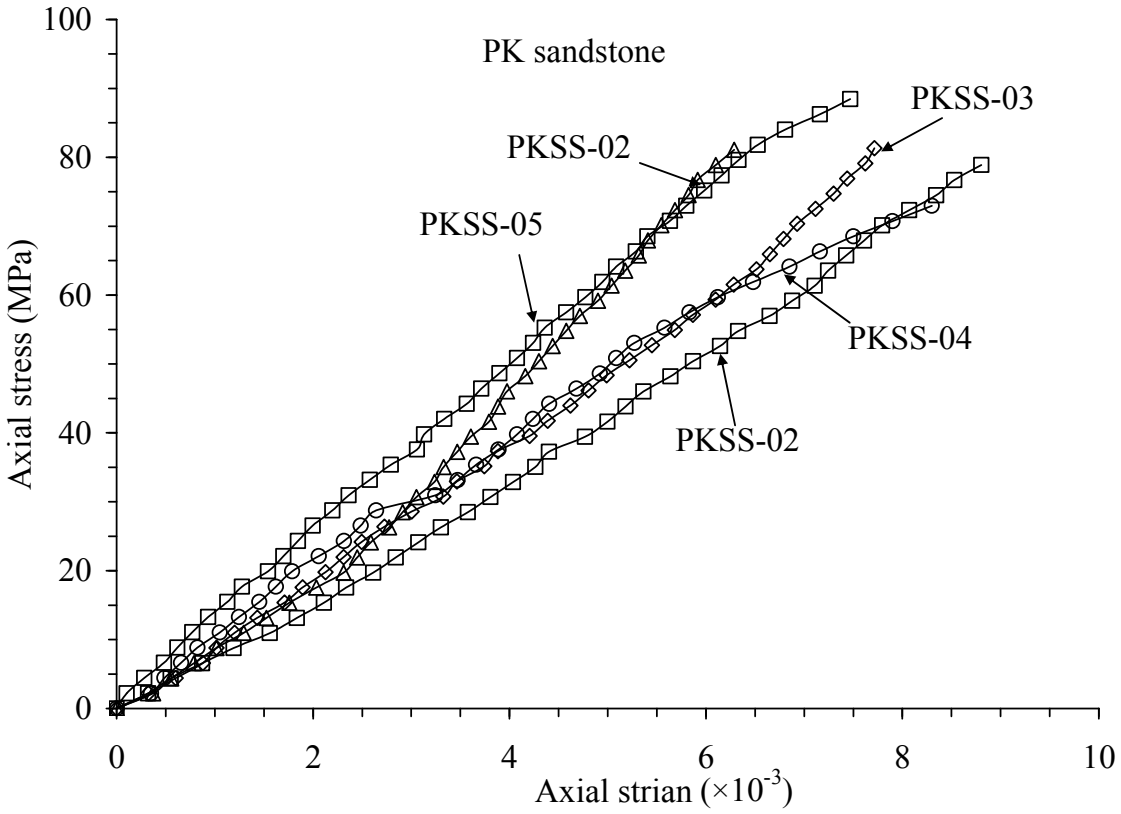

Figure 4.4 Results of uniaxial compressive strength tests of PK sandstone. The axial stresses are plotted as a function of axial strain.

a constant loading rate. The failures occur within 5-15 minute of loading under each confining pressure.

The results of the triaxial compressive tests are shown in Table 4.2. Figures 4.5 through 4.7 show the Mohr circles of the results with shear stress as ordinates and normal stress as abscissas. The relationship can be represented by the Coulomb criterion;

$$\tau = c + \sigma_n \tan\phi \qquad (4.1)$$

where τ is the shear stress, c is the cohesion, σ_n is the normal stress and ϕ is the angle of internal friction.

Table 4.2 Strength properties from conventional triaxial compression tests.

Types	Specimen No.	Length (mm)	Diameter (mm)	Density (g/cc)	Confining Pressure, σ_3 (MPa)	Axial Stress, σ_1 (MPa)
PW	PWSS-01	106.20	53.90	2.63	1.7	79.4
	PWSS-02	107.30	53.90	2.64	3.4	101.0
	PWSS-03	106.70	53.90	2.63	5.2	107.8
	PWSS-04	107.26	53.90	2.62	6.9	120.6
	PWSS-05	106.48	53.90	2.61	10.3	184.2
	Cohesion, c (MPa)				**10**	
	Friction Angles, ϕ (degrees)				**58**	
PP	PPSS-01	107.50	53.90	2.63	1.7	103.2
	PPSS-02	106.35	53.90	2.64	3.4	134.0
	PPSS-03	106.70	53.90	2.63	5.2	172.5
	PPSS-04	107.82	53.90	2.62	6.9	191.3
	PPSS-05	108.00	53.90	2.61	10.3	205.8
	Cohesion, c (MPa)				**20**	
	Friction Angles, ϕ (degrees)				**52**	
PK	PKSS-01	107.26	53.90	2.61	1.7	107.2
	PKSS-02	106.35	53.90	2.61	3.4	120.5
	PKSS-03	105.50	53.90	2.62	5.2	127.6
	PKSS-04	106.28	53.90	2.6	6.9	129.1
	PKSS-05	107.00	53.90	2.63	10.3	173.2
	Cohesion, c (MPa)				**19**	
	Friction Angles, ϕ (degrees)				**50**	

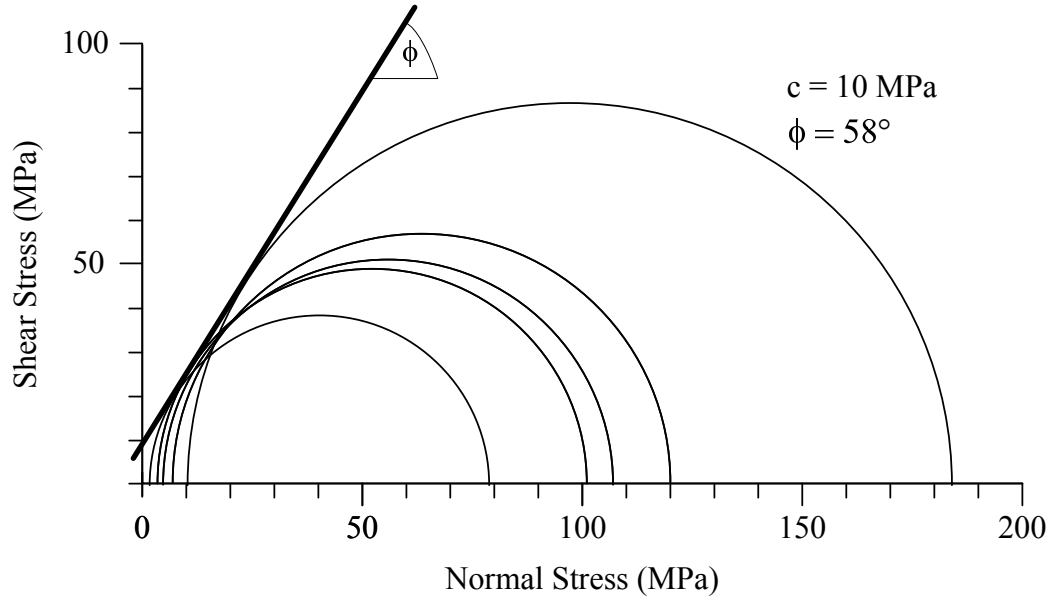

Figure 4.5 Results of triaxial compressive strength tests on Phra Wihan sandstone in form of Mohr's circles and Coulomb criterion.

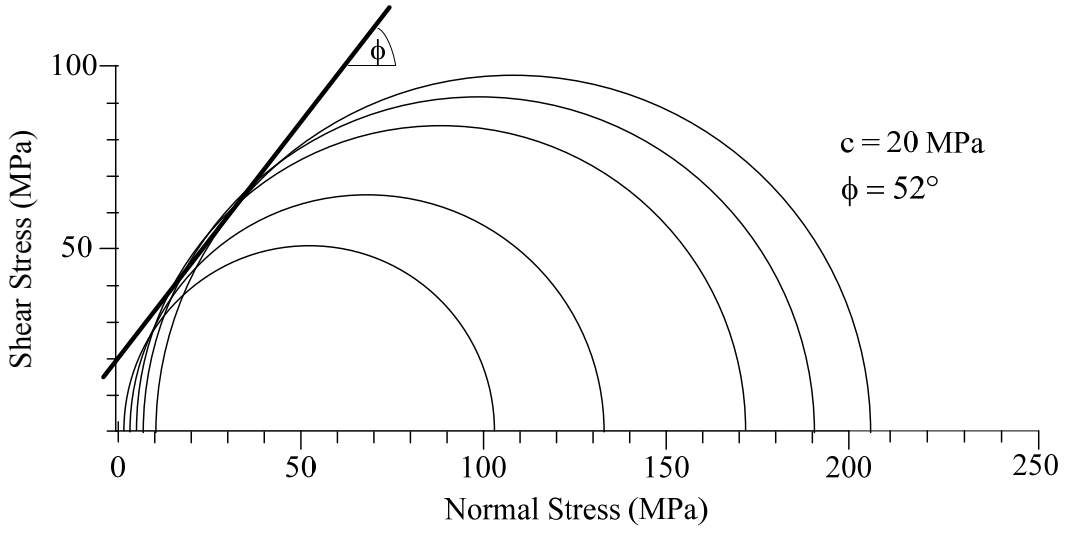

Figure 4.6 Results of triaxial compressive strength tests on Phu Phan sandstone in form of Mohr's circles and Coulomb criterion.

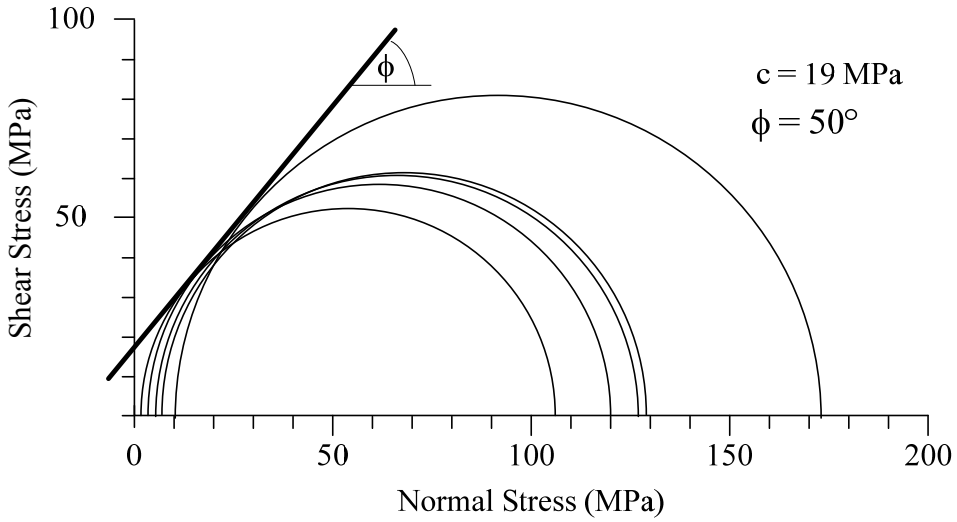

Figure 4.7 Results of triaxial compressive strength tests on Phu Kradung sandstone in form of Mohr's circles and Coulomb criterion.

4.3 Polyaxial compressive strength tests

The polyaxial compression tests are performed to determine the compressive strengths and deformations of the PK, PP and PW sandstones under true triaxial stresses. The intermediate (σ_2) and minimum (σ_3) principal stresses are maintained constant while σ_1 is increased until failure. Here the constant σ_2 is varied from 0 to 17 MPa, and σ_3 from 0 to 6 MPa. Neoprene sheets are used to minimize the friction at all interfaces between the loading platen and the rock surface. Figure 4.8 shows the applied principal stress directions with respect to the bedding planes for all specimens. The failure stresses are recorded and mode of failure examined. Figure 4.9 shows the polyaxial load frame used in this test. To meet the load requirement above, two pairs of cantilever beams are used to apply the lateral stresses in mutually perpendicular directions to the rock specimen. The outer end of each opposite beam is pulled down by dead weight placed in the middle of a steel bar linking the two opposite beams

underneath (Figure 4.10). The inner end is hinged by a pin mounted on vertical bars on each side of the frame. During testing all beams are arranged perfectly horizontally, and hence a lateral compressive load results on the specimen placed at the center of the frame. Due to the different distances from the pin to the outer weighting point and from the pin to the inner loading point.

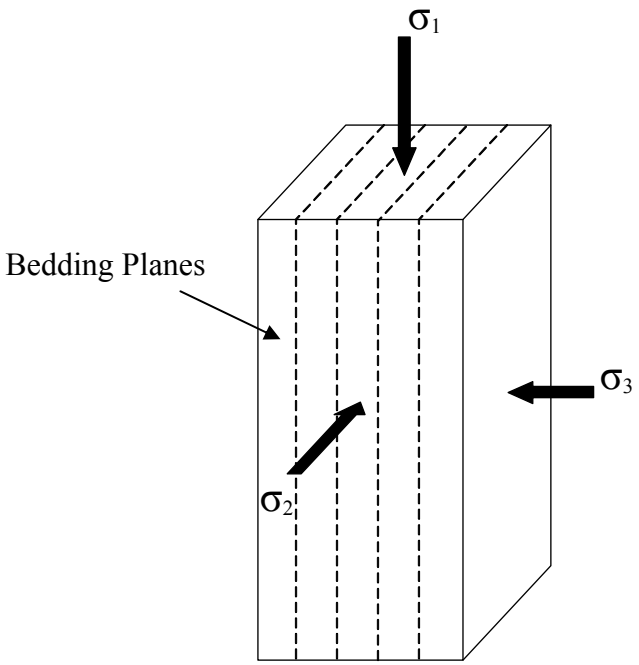

Figure 4.8 Directions of loading with respect to the bedding planes.

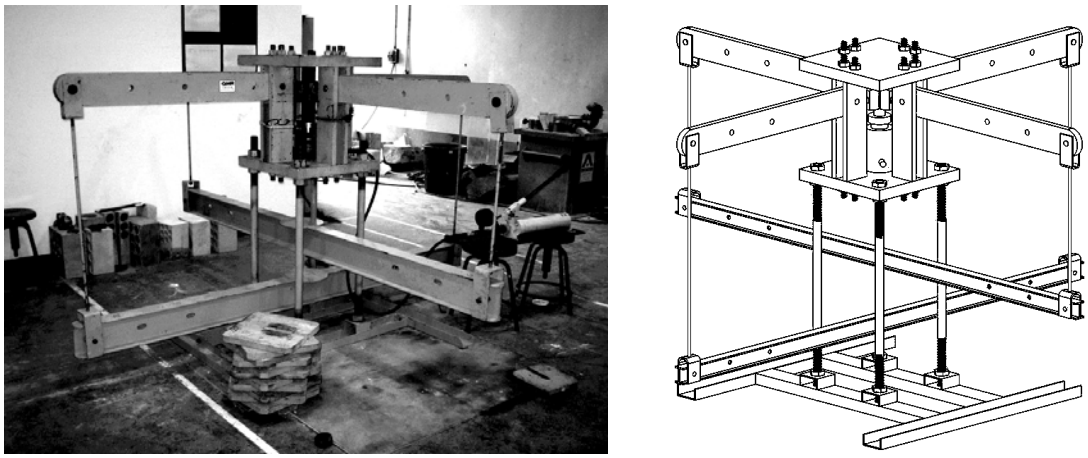

Figure 4.9 Polyaxial load frame developed for compressive and tensile strength testing under true triaxial stress (Walsri et al., 2009).

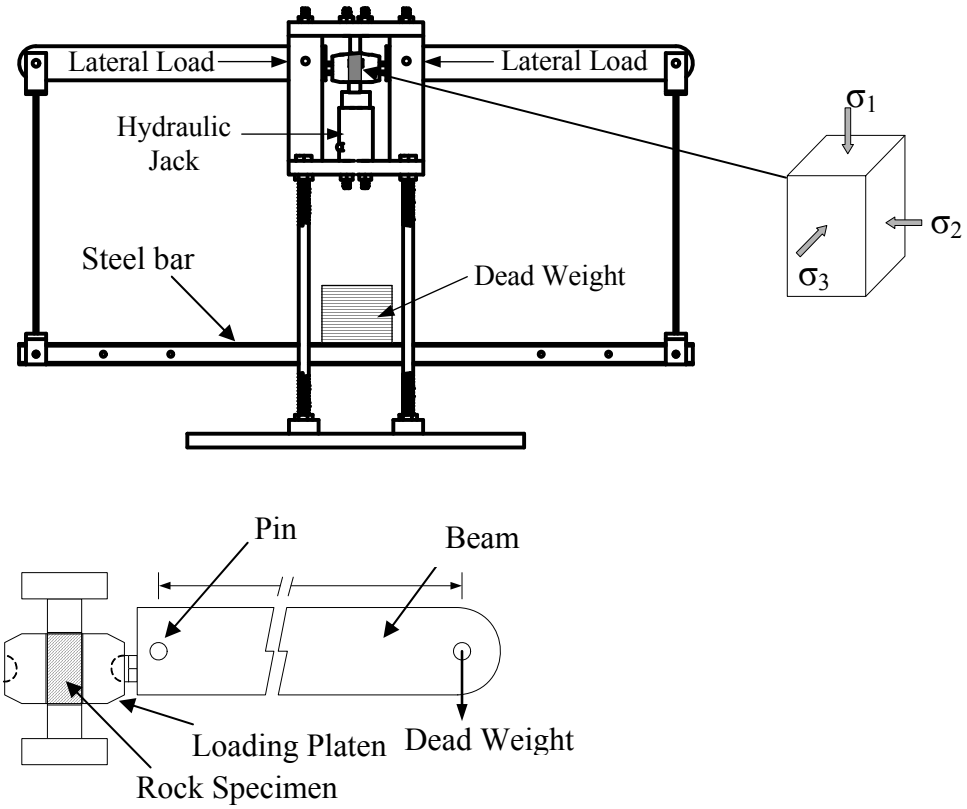

Figure 4.10 Cantilever beam weighed at outer end applies lateral stress to the rock specimen (Walsri et al., 2009).

4.4 Test results

Table 4.3 through 4.5 summarizes the test results on PP, PW and PK sandstones. Figures 4.11 through 4.13 plot σ_1 at failure as a function of σ_2 tested under various σ_3's for the PW, PP and PK sandstones. For all types of sandstone, the results show the effects of the intermediate principal stress, σ_2, on the maximum stresses at failure by the failure envelopes being offset from the condition where $\sigma_2 = \sigma_3$. For all minimum principal stress levels, σ_1 at failure increases with σ_2. The effect of σ_2 tends to be more pronounced under a greater σ_3. These observations agree with those obtained elsewhere (e.g. Haimson and Chang, 2000; Colmenares and Zoback, 2002; Haimson, 2006). Post-failure observations suggest that compressive shear failures are predominant in the specimens tested under low σ_2 while splitting tensile fractures parallel to σ_1 and σ_2 directions dominate under higher σ_2 (Figures 4.14 through 4.16).

Table 4.3 Summary f test results from of Phra Wihan sandstones under true triaxial compressive strength testing.

Types	Sample No.	Area (cm^2)	σ_3 (MPa)	Area (cm^2)	σ_2 (MPa)	Area (cm^2)	σ_1 (MPa)
PW Sandstone	PW-PX-03	0.60	0.0	0.60	0.0	0.3	48.5
	PW-PX-15	0.52	0.0	0.54	3.0	0.3	50.5
	PW-PX-59	0.55	0.0	0.52	6.6	0.3	51.8
	PW-PX-43	0.52	0.0	0.52	10.1	0.3	60.8
	PW-PX-61	0.56	0.0	0.52	17.6	0.3	63.7
	PW-PX-48	0.53	0.0	0.53	24.0	0.3	60.7
	PW-PX-46	0.52	3.0	0.54	3.0	0.3	95.9
	PW-PX-53	0.52	3.0	0.52	6.6	0.3	104.5
	PW-PX-49	0.51	3.0	0.51	10.1	0.3	103.4
	PW-PX-55	0.54	3.0	0.53	17.6	0.3	127.5
	PW-PX-56	0.56	6.6	0.51	6.6	0.3	134.2
	PW-PX-57	0.56	6.6	0.54	10.1	0.3	135.1
	PW-PX-58	0.53	6.6	0.52	13.8	0.3	149.8
	PW-PX-59	0.55	6.6	0.52	17.6	0.3	159.1

Table 4.4 Summary of test results from of Phu Phan sandstones under true triaxial compressive strength testing.

Types	Sample No.	Area (cm^2)	σ_3 (MPa)	Area (cm^2)	σ_2 (MPa)	Area (cm^2)	σ_1 (MPa)
PP Sandstone	PP-PX-03	0.53	0.0	0.55	0.0	0.3	49.4
	PP-PX-05	0.52	0.0	0.53	3.0	0.3	77.2
	PP-PX-09	0.54	0.0	0.54	6.6	0.3	83.8
	PP-PX-10	0.54	0.0	0.54	10.1	0.3	93.4
	PP-PX-15	0.53	0.0	0.54	17.6	0.3	103.3
	PP-PX-38	0.54	0.0	0.54	24.0	0.3	76.3
	PP-PX-22	0.54	3.0	0.54	3.0	0.3	113.1
	PP-PX-23	0.54	3.0	0.54	6.6	0.3	123.8
	PP-PX-24	0.50	3.0	0.50	10.1	0.3	127.3
	PP-PX-32	0.54	3.0	0.54	17.6	0.3	135.8
	PP-PX-29	0.53	6.6	0.53	6.6	0.3	144.0
	PP-PX-33	0.54	6.6	0.54	10.1	0.3	152.5
	PP-PX-35	0.53	6.6	0.54	13.8	0.3	165.9
	PP-PX-36	0.54	6.6	0.54	17.6	0.3	163.9

Table 4.5 Summary of test results from of Phu Kadung sandstones under true triaxial compressive strength testing.

Types	Sample No.	Area (cm^2)	σ_3 (MPa)	Area (cm^2)	σ_2 (MPa)	Area (cm^2)	σ_1 (MPa)
PK Sandstone	PK-PX-13	0.52	0.0	0.54	0.0	0.3	46.4
	PK-PX-10	0.54	0.0	0.52	3.0	0.3	56.9
	PK-PX-11	0.53	0.0	0.53	6.6	0.3	60.8
	PK-PX-12	0.53	0.0	0.53	10.1	0.3	71.5
	PK-PX-13	0.54	0.0	0.55	17.6	0.3	75.0
	PK-PX-21	0.52	0.0	0.53	24.0	0.3	78.9
	PK-PX-05	0.51	3.0	0.52	3.0	0.3	76.9
	PK-PX-14	0.53	3.0	0.51	6.6	0.3	93.0
	PK-PX-16	0.53	3.0	0.54	10.1	0.3	94.9
	PK-PX-17	0.52	3.0	0.53	17.6	0.3	106.6
	PK-PX-18	0.53	6.6	0.52	6.6	0.3	123.8
	PK-PX-19	0.54	6.6	0.53	10.1	0.3	128.2
	PK-PX-23	0.53	6.6	0.54	13.8	0.3	137.7
	PK-PX-20	0.54	6.6	0.53	17.6	0.3	147.6

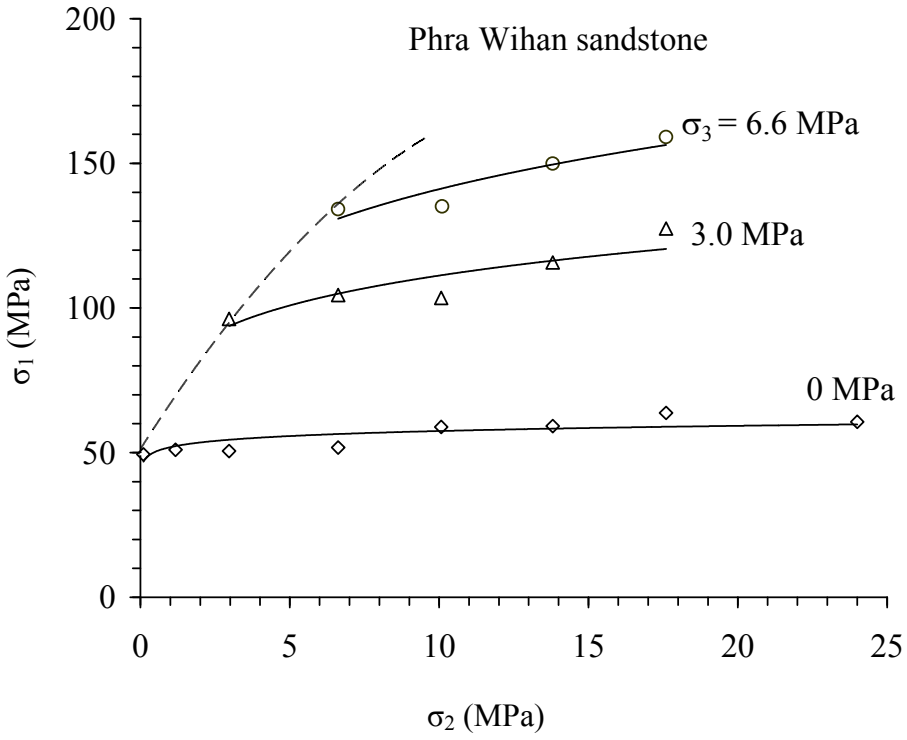

Figure 4.11 Maximum principal stress (σ_1) at failure as a function of σ_2 for various σ_3 values for Phra Wihan sandstone.

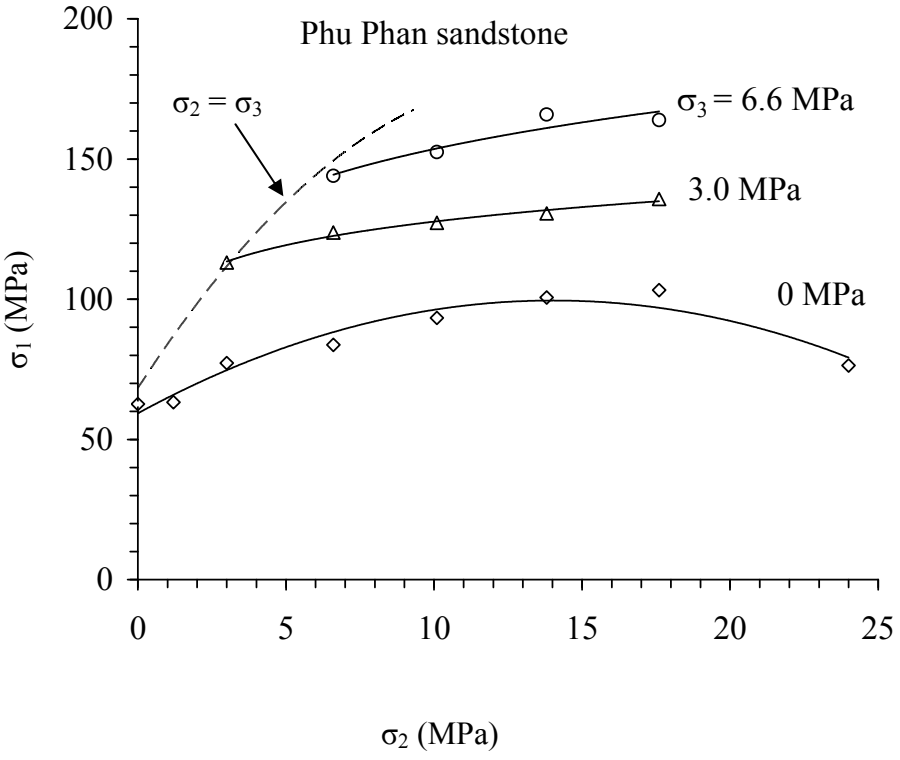

Figure 4.12 Maximum principal stress (σ_1) at failure as a function of σ_2 for various σ_3 values for Phu Phan sandstone.

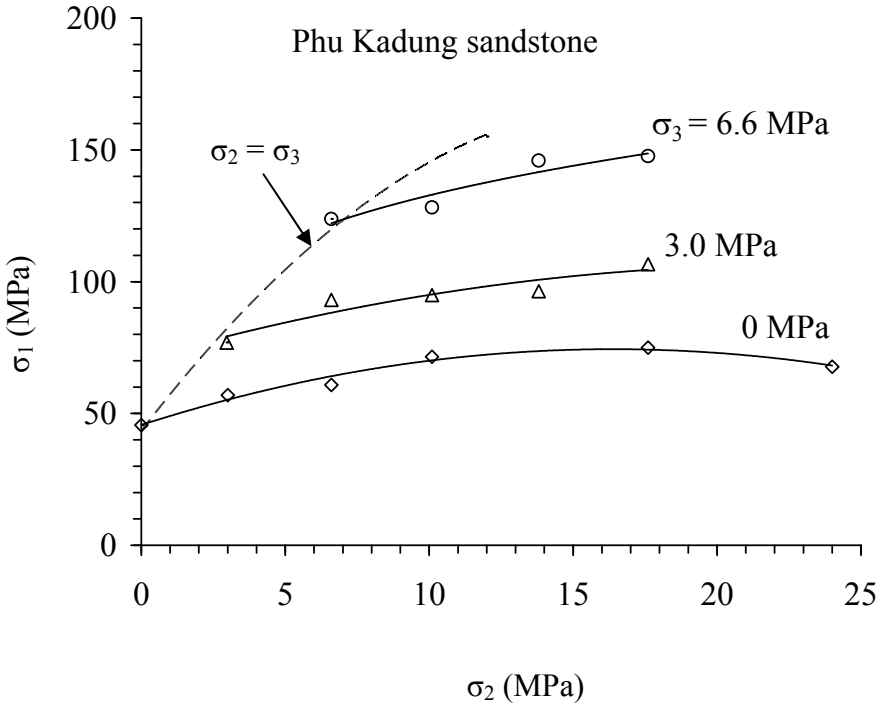

Figure 4.13 Maximum principal stress (σ_1) at failure as a function of σ_2 for various σ_3 values for Phu Kadung sandstone.

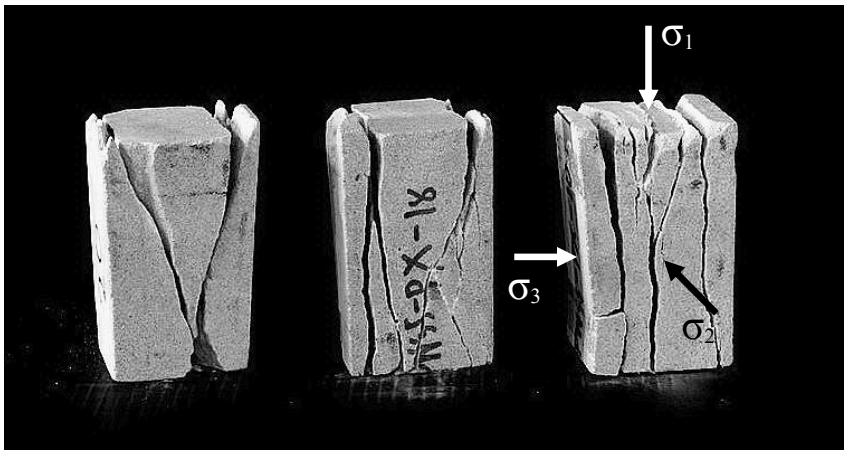

Figure 4.14 Post-test specimens of Phra Wihan sandstone. Left: σ_1 = 50.5, σ_2 = 3.0, σ_3 = 0 MPa. Middle: σ_1 = 51.8, σ_2 = 6.6, σ_3 = 0 MPa. Right: σ_1 = 60.8, σ_2 = 10.0, σ_3 = 0 MPa.

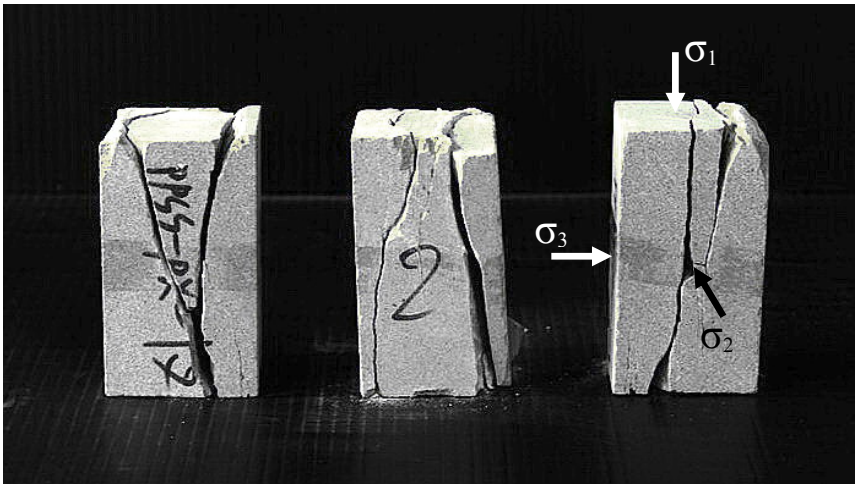

Figure 4.15 Post-tested specimens of Phu Phan sandstone. Left: σ_1 = 77.2, σ_2 = 3.0, σ_3 = 0 MPa. Middle: σ_1 = 83.8, σ_2 = 6.6, σ_3 = 0 MPa. Right: σ_1 = 93.4, σ_2 = 10.0, σ_3 = 0 MPa.

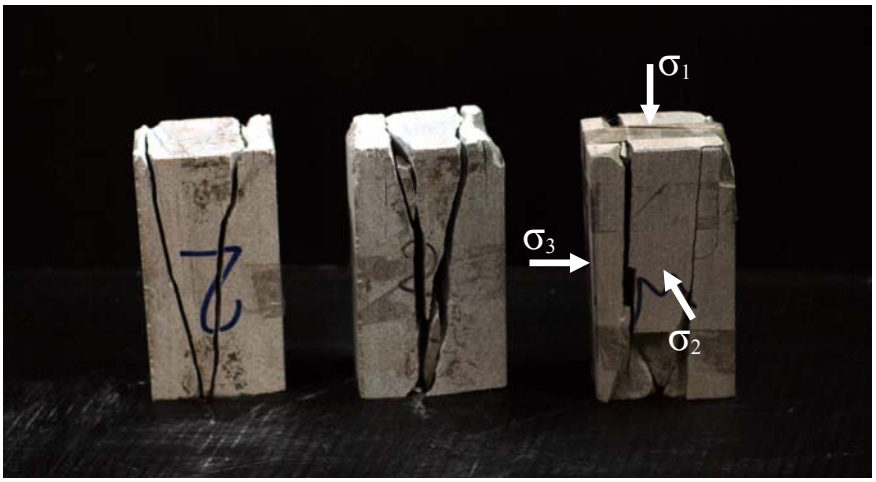

Figure 4.16 Post-tested specimens of Phu Kadung sandstone. Left: σ_1 = 56.9, σ_2 = 3.0, σ_3 = 0 MPa. Middle: σ_1 = 60.8, σ_2 = 6.6, σ_3 = 0 MPa. Right: σ_1 = 71.5, σ_2 = 10.0, σ_3 = 0 MPa.

The observed splitting tensile fractures under relatively high σ_2 suggest that the fracture initiation has no influence from the friction at the loading interface in the σ_2 direction. As a result the increase of σ_1 with σ_2 should not be due to the interface friction. This does not agree with a conclusion drawn by Cai (2008) that friction at the interface in the σ_2 direction contributes to the increase of σ_1 at failure. Under the conditions when $\sigma_2 = \sigma_3$, the magnitudes of σ_1 at failure agree well with the triaxial compressive strength test results obtained by Kenkhunthod and Fuenkajorn (2009).

Table 4.6 compares the uniaxial compressive strength and triaxial compressive strength tests with true triaxial compressive strength test. Conditions of testing are that the intermediate principal stress equals the minimum principal stresses. Results of the triaxial compressive strength tests are higher than the true triaxial compressive strength tests. This may be because the shapes of the specimens are different.

Table 4.6 Comparisons of results between conventional triaxial compressive strength tests and true triaxial compressive strength tests.

Type	$\sigma_2 = \sigma_3$ (MPa)	Conventional Triaxial Test (MPa)	True Triaxial Test (MPa)
PW Sandstone	0	65.7	48.5
	3	101.0	95.9
	6.6	120.6	134.2
PP Sandstone	0	76.8	49.4
	3	134.0	113.1
	6.6	191.3	144.0
PK Sandstone	0	60.5	46.4
	3	120.5	76.9
	6.6	129.1	123.8

CHAPTER V

STRENGTH CRITERIA

5.1 Introduction

This chapter describes the strength analysis and criteria under true triaxial compression. The test results are compared with the Coulomb and modified Wiebols and Cook failure criteria. They are selected because the Coulomb criterion has been widely used in actual field applications while the modified Wiebols and Cook criterion has been claimed by many researchers to be one of the best representations of rock strengths under confinement.

5.2 Coulomb criterion prediction

The second order stress invariant ($J_2^{1/2}$) and the first order stress invariant or the mean stress (J_1) is calculated from the test results by the following relations (Jaeger and Cook, 1979):

$$J_2^{1/2} = \sqrt{(1/6)\{(\sigma_1 - \sigma_2)^2 + (\sigma_1 - \sigma_3)^2 + (\sigma_2 - \sigma_3)^2\}} \tag{5.1}$$

$$J_1 = (\sigma_1 + \sigma_2 + \sigma_3)/3 \tag{5.2}$$

The Coulomb criterion in from of J_2 and J_1 can be expressed as (Jaeger and Cook, 1979):

$$J_2^{1/2} = \frac{2}{\sqrt{3}}\left[J_1 \sin\varphi + S_0 \cos\phi\right] \tag{5.3}$$

where ϕ is friction angle, S_o is cohesion, J_1 is mean stress and $J_2^{1/2}$ is the second order of stress invariant. Table 5.1 shows the results of the strength calculation in terms of $J_2^{1/2}$ and J_1 for all sandstones. From the test results the stress invariant $J_2^{1/2}$ as a function of mean stress J_1 is compared with the predictions by the Coulomb criterion in Figures 5.1 through 5.3 for PP, PW and PK sandstones. The prediction uses ϕ and S_0. There values are obtained from the characterization testing (given in chapter 4). Since the Coulomb criterion ignores σ_2 at failure, the predicted $J_2^{1/2}$ is independent of J_1 for each σ_3. Under a low σ_2 and σ_3 the Coulomb prediction tends to agree with the test results obtained from the PW sandstone. Except for this case, no correlation between the Coulomb predictions and the polyaxial strengths can be found. The inadequacy of the predictability of Coulomb criterion under polyaxial stress states obtained here agrees with a conclusion drawn by Colmenares and Zoback (2002).

5.3 Modified Wiebols and Cook criteria prediction

The modified Wiebols and Cook criterion given by Colmenares and Zoback (2002) defines $J_2^{1/2}$ at failure in terms of J_1 as:

$$J_2^{1/2} = A + BJ_1 + CJ_1^2 \tag{5.4}$$

The constants A, B and C depend on rock materials and the minimum principal stresses (σ_3). They can be determined under the conditions where $\sigma_2 = \sigma_3$, as follows (Colmenares and Zoback, 2002):

$$C = \frac{\sqrt{27}}{2C_1 + (q-1)\sigma_3 - C_0} \times \left(\frac{C_1 + (q-1)\sigma_3 - C_0}{2C_1 + (2q+1)\sigma_3 - C_0} - \frac{q-1}{q+2} \right) \tag{5.5}$$

Table 5.1 Strength calculation in terms of $J_2^{1/2}$ and J_1.

Sandstones	σ_3 (MPa)	σ_2 (MPa)	σ_1 (MPa)	J_1 (MPa)	$J_2^{1/2}$ (MPa)
PW	0.0	0	48.5	16.5	28.5
		3.0	50.5	17.8	28.4
		6.6	51.8	19.5	28.2
		10.1	60.8	23.0	31.5
		17.6	63.7	27.1	32.9
		24.0	60.7	28.2	30.6
	3.0	3.0	95.9	33.9	53.5
		6.6	104.5	38.0	57.6
		10.1	103.4	38.9	56.1
		17.6	127.5	49.4	68.0
	6.6	6.6	134.2	49.1	73.7
		10.1	135.1	50.6	73.2
		13.8	149.8	56.8	80.8
		17.6	159.1	61.1	85.1
PP	0.0	0	49.4	20.9	36.2
		3.0	77.2	26.7	43.7
		6.6	83.8	30.1	46.6
		10.1	93.4	34.5	51.2
		17.6	103.3	40.3	55.3
		24.0	76.3	33.4	39.0
	3.0	3.0	113.1	39.7	63.6
		6.6	123.8	44.5	68.7
		10.1	127.3	46.8	69.8
		17.6	135.8	52.1	72.8
	6.6	6.6	144.0	52.4	79.4
		10.1	152.5	56.4	83.2
		13.8	165.9	62.1	90.0
		17.6	163.9	62.7	87.8
PK	0.0	0	46.4	15.2	26.3
		3.0	56.9	20.0	32.0
		6.6	60.8	22.5	33.4
		10.1	71.5	27.2	38.7
		17.6	75.0	28.5	35.2
		24.0	78.9	30.6	34.3
	3.0	3.0	76.9	27.6	42.6
		6.6	93.0	34.2	51.0
		10.1	94.9	36.0	51.1
		17.6	106.6	42.4	56.1
	6.6	6.6	123.8	45.7	67.7
		10.1	128.2	48.3	69.2
		13.8	137.7	52.7	73.7
		17.6	147.6	57.3	78.4

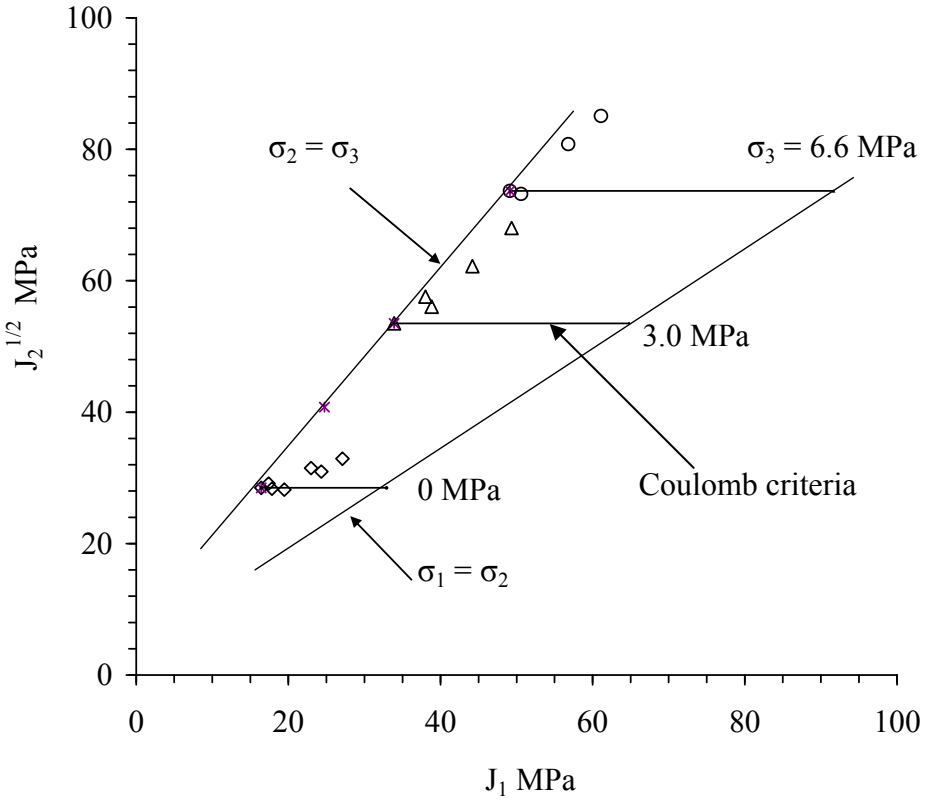

Figure 5.1 $J_2^{1/2}$ as a function of J_1 for true triaxial compression testing on PW sandstones compared with the Coulomb criterion predictions, for σ_3 = 0, 3.0 and 6.6 MPa.

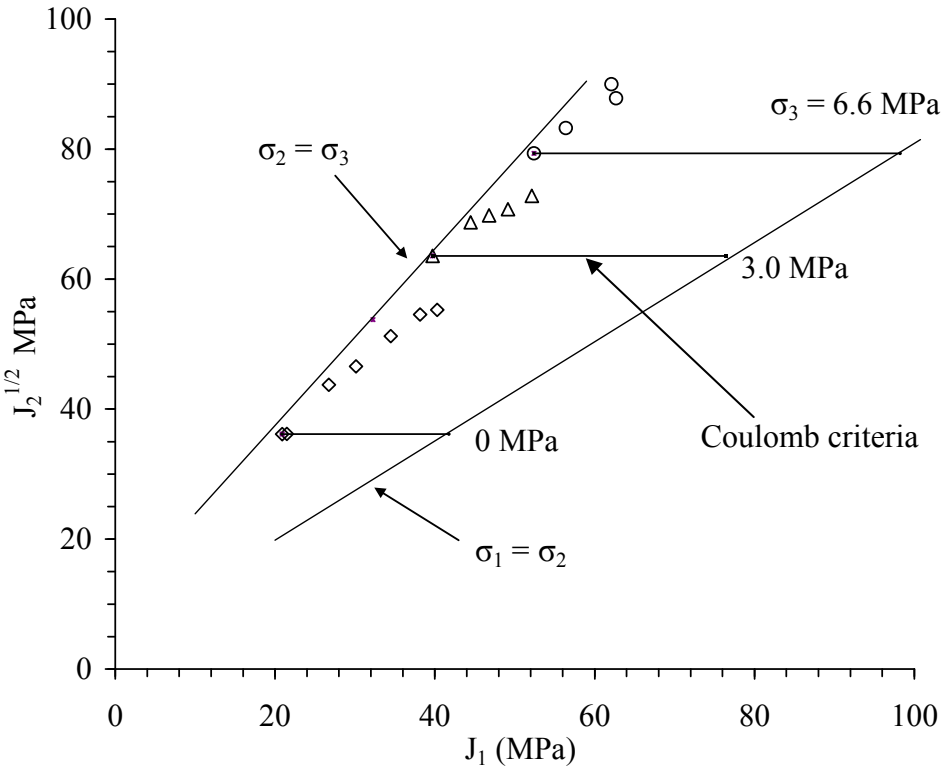

Figure 5.2 $J_2^{1/2}$ as a function of J_1 for true triaxial compression testing on PP sandstones compared with the Coulomb criterion predictions, for σ_3 = 0, 3.0 and 6.6 MPa.

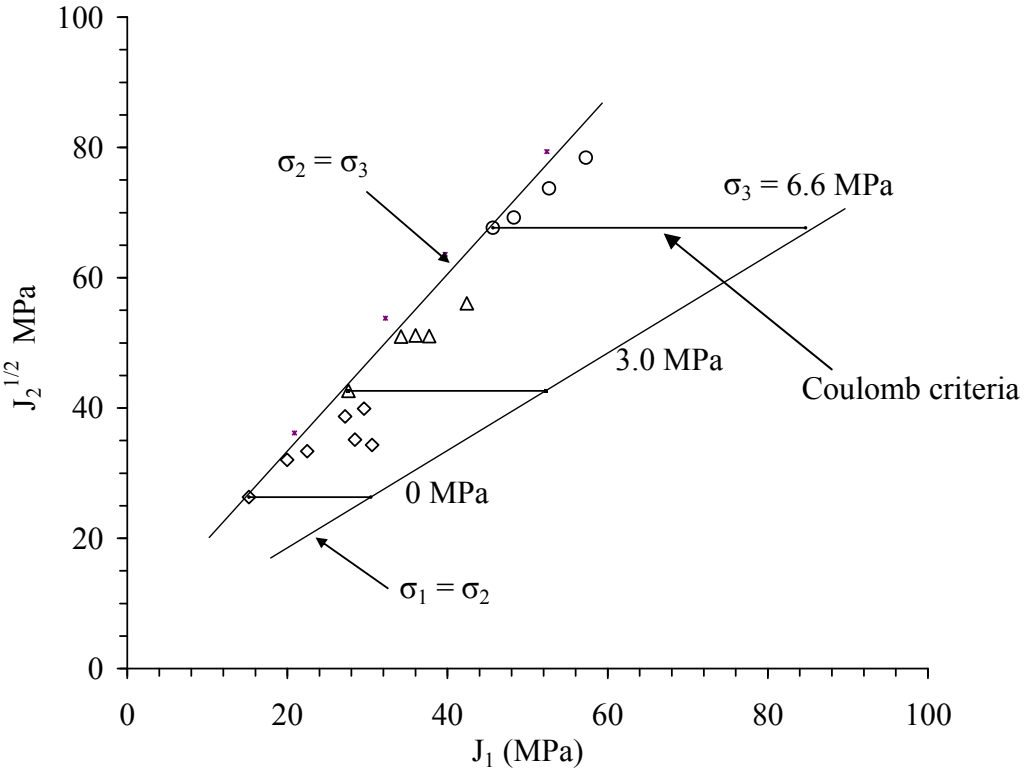

Figure 5.3 $J_2^{1/2}$ as a function of J_1 for true triaxial compression testing on PK sandstones compared with the Coulomb criterion predictions, for σ_3 = 0, 3.0 and 6.6 MPa.

where: $C_1 = (1 + 0.6\mu_i)C_0$

C_0 = uniaxial compressive strength of the rock

$\mu_i = \tan\phi$

$$q = \{(\mu_i^2 + 1)^{1/2} + \mu_i\}^2 = \tan^2(\pi/4 + \phi/2)$$

$$B = \frac{\sqrt{3}(q-1)}{q+2} - \frac{C}{3}(2C_0 + (q+2)\sigma_3 \qquad (5.6)$$

$$A = \frac{C_0}{\sqrt{3}} - \frac{C_0}{3}B - \frac{{C_0}^2}{9}C \tag{5.7}$$

The comparison between the measured strengths with the predictions by the modified Wiebols and Cook criterion for the three sandstones are given in Figures 5.4 through 5.6.

5.4 Discussions of the test results

Under true triaxial compressive stresses the modified Wiebols and Cook criterion can predict the compressive strengths of the tested sandstones reasonably well. This agrees with the results obtained by Haimson (2000) and Colmenares and Zoback (2002). Due to the effect of σ_2 the Coulomb criterion can not represent the rock strengths under true triaxial compressions, particularly under high σ_2 to σ_3 ratios. This is because the Coulomb criterion ignores the intermediate principal stress in the calculation of stress state at failure.

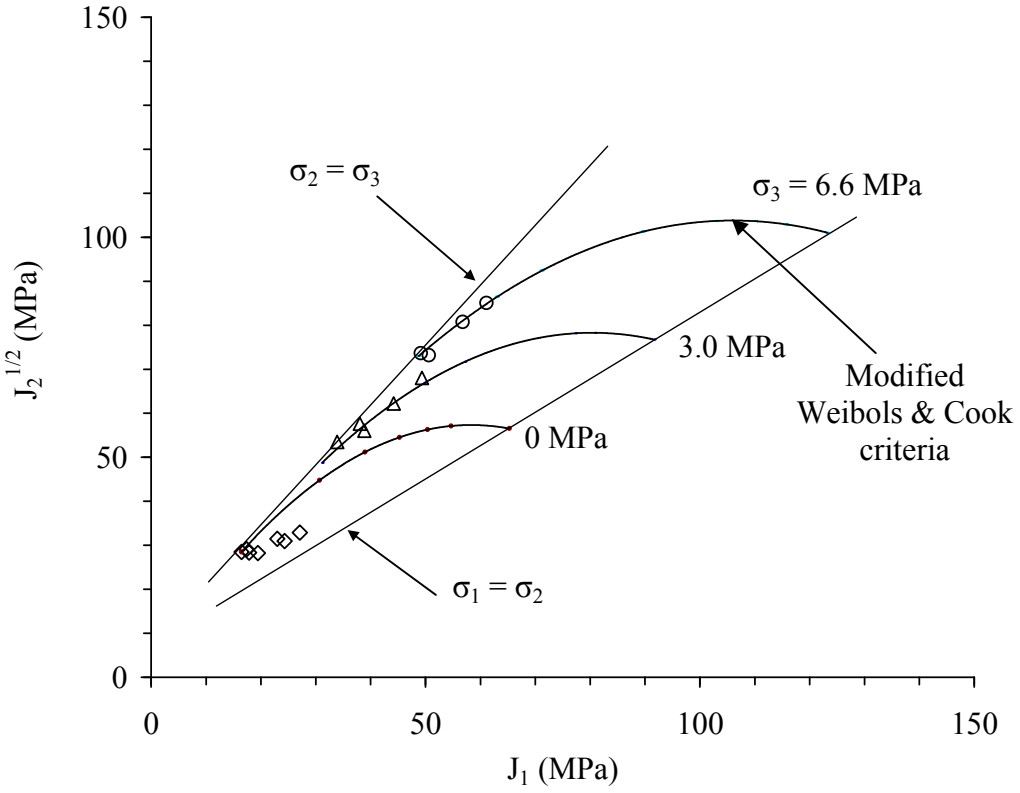

Figure 5.4 $J_2^{½}$ as a function of J_1 for true triaxial compression testing on PW sandstones compared with the modified Wiebols and Cook criterion, for σ_3 = 0, 3.0 and 6.6 MPa.

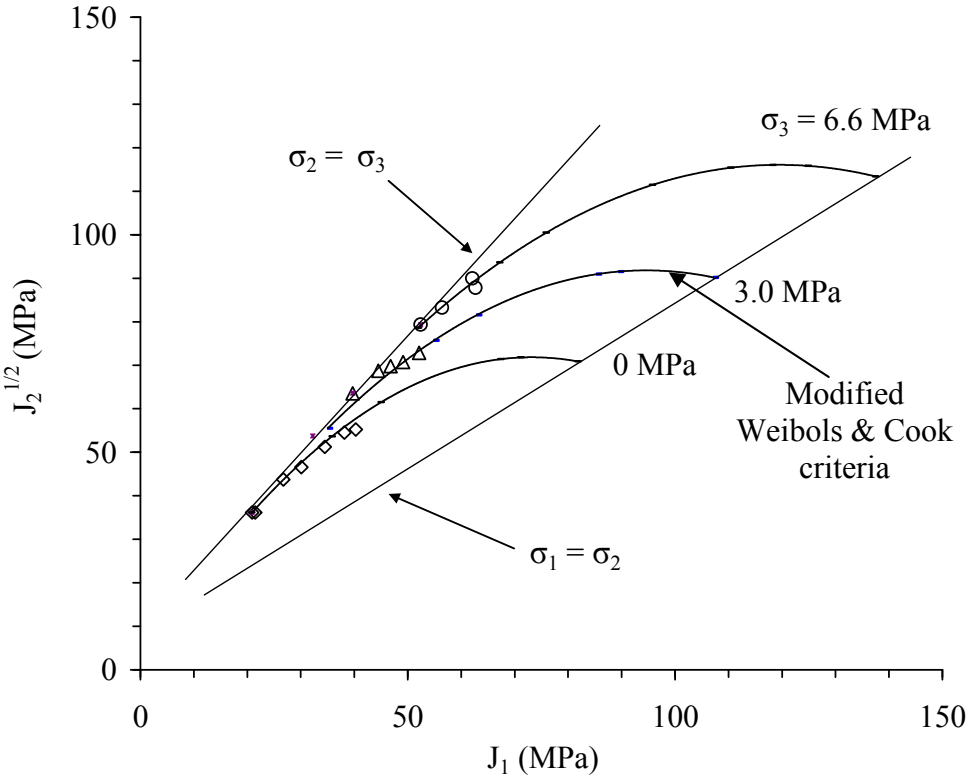

Figure 5.5 $J_2^{½}$ as a function of J_1 for true triaxial compression testing on PP sandstones compared with the modified Wiebols and Cook criterion, for σ_3 = 0, 3.0 and 6.6 MPa.

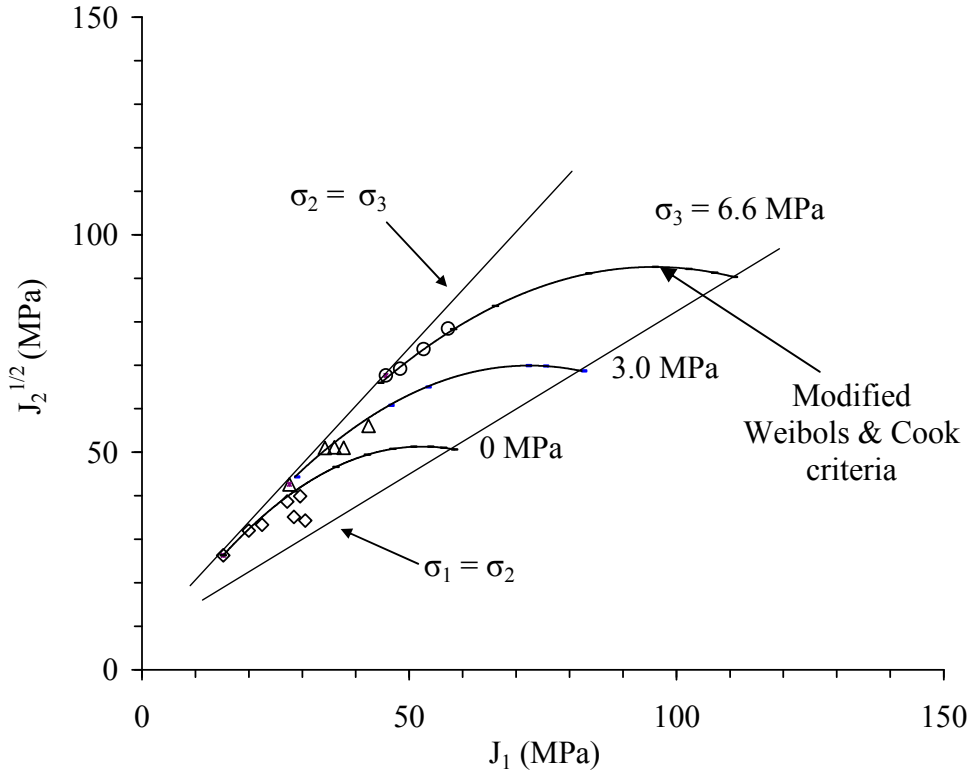

Figure 5.6 $J_2^{1/2}$ as a function of J_1 for true triaxial compression testing on PK sandstones compared with the modified Wiebols and Cook criterion, for σ_3 = 0, 3.0 and 6.6 MPa.

CHAPTER VI

DISCUSSIONS, CONCLUSIONS, AND RECOMMENDATIONS FOR FUTURE STUDIES

6.1 Discussions and conclusions

True triaxial compressive strengths of PW, PP and PK sandstones have been determined in this study. Rectangular specimens with a nominal dimension of $5\times5\times10$ cm^3 are prepared. A polyaxial load frame equipped with cantilever beam is used to apply constant σ_2 and σ_3 while σ_1 (along the long axis is increased until failure. The strength results clearly show that σ_2 affects the maximum stress, σ_1 at failure for all sandstones. This phenomenon agrees with those observed elsewhere. Under true triaxial compressive stresses the modified Wiebols and Cook criterion can predict the compressive strengths of the tested sandstones reasonably well. Due to the effect of σ_2 the Coulomb criterion can not represent the rock strengths under true triaxial compressions, particularly under high σ_2 to σ_3 ratios.

It is postulated that the effects of the intermediate principal stress are caused by two mechanisms working simultaneously but having opposite effects on the rock polyaxial strengths; (1) mechanism that strengthens the rock matrix in the direction normal to σ_1 - σ_3 plane, and (2) mechanism that induces tensile strains in the directions of σ_1 and σ_3. The intermediate principal stress can strengthen the rock matrix on the plane normal to its direction, and hence a higher differential stress is required to induce failure. This is the same effect obtained when applying a confining pressure to a

cylindrical specimen in the conventional triaxial compression testing. Considering this effect alone, the higher the magnitude of σ_2 applied, the higher σ_1 (or $J_2^{1/2}$) is required to fail the specimen. Nevertheless it is believed that the relationship between σ_2 magnitudes and the degrees of strengthening can be non-linear, particularly under high σ_2. Such relation depends on rock types and their texture (e.g., distribution of grain sizes, pore spaces, fissures and micro-cracks, and types of rock-forming minerals).

6.2 Recommendations for future studies

The uncertainties and adequacies of the research investigation and results discussed above lead to the recommendations for further studies. More testing is required to assess the effect of the intermediate principal stress. Studying of σ_2 effect on a variety of rocks with a broad range of strengths and elasticity should be conducted. This is to confirm the reliability of the modified Wiebols and Cook criterion. The effects of pore pressure on the rock compressive strengths and elasticity is also desirable. Study of effects of loading rate and time-dependency under polyaxial stresses can also improve our understanding of the rock creep behavior under anisotropic stress states.

REFERENCES

Alexeev, A.D., Revva, V.N., Alyshev, N.A., and Zhitlyonok, D.M. (2004). True triaxial loading apparatus and its application to coal outburst prediction. **International Journal of Coal Geology**. 58: 245-250.

Al-Ajmi, A.M. and Zimmerman, R.W. (2005). Relation between the Mogi and the Coulomb failure criteria. **International Journal of Rock Mechanics and Mining Sciences**. 42: 431-439.

Al-Rawas, A.A., Taha, R., Nelson, J.D., Al-Shap, T.B., and Al-Siyabi, H. (2002). **Geotechnical Testing Journal**. 25: 199-209.

Alsayed, M.I. (2002). Utilising the hoek triaxial cell for multiaxial testing of hollow rock cylinders. **International Journal of Rock Mechanics and Mining Sciences**. 39: 355-366.

Amadei, B. and Robinson, J. (1986). Strength of rock in multi-axial loading conditions. In **Proceedings of the 27th U.S. Symposium on Rock Mechanics**. Tuscaloosa, Alabama, pp. 47-55.

Anhdan, L.Q., Koseki, J., Hayano, K., and Sato, T. (2005). True triaxial apparatuses with two rigid boundaries. **Geo-Frontiers 2005**. 18: 1-34.

ASTM D4543-85. Standard Practice for Preparing Rock Core Specimens and Determining Dimensional and Shape Tolerances. **In Annual Book of ASTM Standards** (Vol. 04.08). Philadelphia: American Society for Testing and Materials.

ASTM D7012-04. Test Method for Compressive Strength and Elastic Moduli of Intact Rock Core Specimens under Varying States of Stress and Temperatures. **In Annual Book of ASTM Standards** (Vol. 04.09). Philadelphia: American Society for Testing and Materials.

Benz, T. and Schwab, R. (2008). A quantitative comparison of six rock failure criteria. **International Journal of Rock Mechanics and Mining Sciences**. 45: 1176-1186.

Brace, W.F. (1964). Brittle fracture of rocks. **In State of stress in the earth''s crust**. Elsevier, N.Y., pp. 111-174.

Brook, N. (1993). The measurement and estimation of basic rock strength. **In J.A. Hudson, Editor, Comprehensive Rock Engineering: Principles, Practices, and Projects**. Oxford: Pergamon Press. 130: 41-66.

Brown, E.T. (1981). **Rock Characterization, Testing and Monitoring - ISRM Suggested Methods**. Oxford: Pergamon.

Cai, M. (2008). Influence of intermediate principal stress on rock fracturing and strength near excavation boundaries—Insight from numerical modeling. **International Journal of Rock Mechanics and Mining Sciences**. 45: 763-772.

Chang, C. and Haimson, B. (2005). Non-dilatant deformation and failure mechanism in two Long Valley Caldera rocks under true triaxial compression. **International Journal of Rock Mechanics and Mining Sciences**. 42: 402-414.

Cheon, D.S., Park, S.J.C., and Ryu, C. (2006). An experimental study on the brittle failure under true triaxial conditions. **Tunnelling and Underground Space Technology**. 21(3-4): 448-449.

Chen, C.H., Pan, E., and Amadei B. (1998). Determination of the deformability and tensile strength of anisotropic rocks using Brazilian tests. **International Journal of Rock Mechanics and Mining Sciences**. 35: 43-61.

Claesson, J. and Bohloli, B. (2002). Brazilian test: stress field and tensile strength of anisotropic rocks using an analytical solution. **International Journal of Rock Mechanics and Mining Sciences**. 14: 991-1004.

Colmenares, L.B. and Zoback, M.D. (2002). A statistical evaluation of intact rock failure criteria constrained by polyaxial test data for five different rocks. **International Journal of Rock Mechanics and Mining Sciences**. 39: 695-729.

Cornet, F.H. (1993). Stresses in rock and rock masses. **In J.A. Hudson, Editor, Comprehensive Rock Engineering: Principles, Practices, and Projects**. Oxford: Pergamon Press. 3: 395-412.

Cheon, D.S., Jeon, S., Park, C., and Ryu, C. (2006). An experimental study on the brittle failure under true triaxial conditions. **Tunnelling and Underground Space Technology**. 21: 448–449.

Dihoru, L., Wood, D.M., Sadek, T., and Lings, M. (2005). A neural network for error prediction in a true triaxial apparatus with flexible boundaries. **Computers and Geotechnics**. 32: 59-71.

Elliott, G.M. (1993). Triaxial testing for rock strength. **In J.A. Hudson, Editor, Comprehensive Rock Engineering: Principles, Practices, and Projects**. Oxford: Pergamon Press. 32: 111-120.

Esaki, T. and Kimura, T. (1989). Mechanical behaviour of rocks under generalized high stress conditions. **In Rock at Great Depth, Maury, V. and Fourmaintraux, D. (eds),** Balkema, Rotterdam. 1: 123-130.

Fakhimi, A., Carvalho, F., Ishida, T., and Labuz, J.F. (2002). Simulation of failure around a circular opening in rock. **International Journal of Rock Mechanics and Mining Sciences**. 39: 507-515.

Franklin, J.A. and Dusseault, M.B. (1989). **Rock Engineering**. McGraw-Hill Inc., U.S.A., pp. 246-247.

Franklin, J.A. and Hoek, E. (1970). Developments in triaxial testing equipment. **Rock Mechanics**. 2: 223-228.

Gau, Q.Q., Cheng, H.T., and Zhuo, D.P. (1983). The strength, deformation and rupture characteristics of red sandstone under polyaxial compression. In **Proceedings of the 5th. International. Congress. Rock Mechanics**. Melbourne, Australia. pp 157-160.

Haimson, B. and Chang, C. (2000). A new true triaxial cell for testing mechanical properties of rock, and its use to determine rock strength and deformability of Westerly granite. **International Journal of Rock Mechanics and Mining Sciences**. 37(1-2): 285-296.

Haimson, B.C., Chang, C., and Chang, C. (2001). True triaxial testing of crystalline rocks reveals new mechanical properties and micromechanics of brittle fracture that go unnoticed in conventional triaxial tests. **American Geophysical Union**, pp. 235-242.

Haimson, B. (2006). True triaxial stresses and the brittle fracture of rock. **Pure and Applied Geophysics**. 163: 1101-1130.

Haimson, B. (2000). A new true triaxial cell for testing mechanical properties of rock, and its use to determine rock strength and deformability of westerly granite. **International Journal of Rock Mechanics and Mining Sciences**. 37: 285-296.

Handin, J., Heard, H.C., and Maguirk, J.N. (1967). Effects of the intermediate principal stress on the failure of limestone, dolomite and glass at different temperatures and strain rates. **Journal of Geophysic Reservoir**. 72: 611-640.

Hoek, E. and Brown, E.T. (1980). Underground excavations in rock. **IMM**. London, pp. 133-136.

Hoek, E. and Franklin, J.A. (1968). A simple triaxial cell for field and laboratory testing of rock. **Transport Instruct Mineral Metallic**. London, Section A. 77: 22-26.

Hojem, J.M.P. and Cook, N.G.W. (1968). The design and construction of a triaxial and polyaxial cell for testing rock specimens. **South African Mechanics Engineering.** 18: 57-61.

Hondros, G. (1959). The evaluation of Poisson's ratio and the modulus of materials of low tensile resistance by the Brazilian (indirect tensile) tests with particular reference to concrete. **Australian Journal of Applied Sciences**. 10: 243-268.

Huang, W., Sun, D., and Sloan, S.W. (2006). Analysis of the failure mode and softening behaviour of sands in true triaxial tests. **International Journal of Solids and Structures**. In Press, Corrected Proof, Available online 22 June 2006. 44: 1423-1437.

Ismail, M.A., Sharma, S.S., and Fahey, M. (2005). A small true Triaxial apparatus with wave velocity measurement. **ASTM International**. West Conshohocken.

Jaeger, J.C. and Cook, N.G.W. (1979). **Fundamentals of Rock Mechanics (3rd. Edn.)**. Chapman and Hall, London, pp. 105-106.

Jianhong, Y., Wu, F.Q., and Sun J.Z. (2008). Estimation of Tensile Elastic Modulus using Brazilian disc by applying diametrically opposed concentrated loads. **International Journal of Rock Mechanics and Mining Sciences**. 46: 568-576.

Joussineau, G.D., Petit, J.P., and Gauthier, B.D.M. (2003). Photoelastic and numerical investigation of stress distributions around fault models under biaxial compressive loading conditions. **Tectnophysics**. 363: 19-43.

Kenkhunthod, N. and Fuenkajorn, K. (2009). Effects of loading rate on compressive strength of sandstones under confinement. In **Proceedings of the Second Thailand Rock Mechanics Symposium**. Nakhon Ratchasima: Suranaree University of Technology. 2: pp 271-282.

Kwaśniewski, M., Takahashi, M., and Li, X. (2003). Volume changes in sandstone under true triaxial compression conditions. **ISRM 2003–Technology Roadmap for Rock Mechanics**. South African Institute of Mining and Metallurgy, pp. 683-688.

Liao, J.J., Yang, M.T., and Hsieh, H.Y. (1997). Direct tensile behavior of a transversely isotropic rock. **International Journal of Rock Mechanics and Mining Sciences**. 34(5): 831-849.

Marsal, R.J. (1973). A true triaxial apparatus to test rockfills. **Defense Technical Information Center**.

Mogi, K. (1970). Effect of triaxial stress system on rock failure. **Rock Mechanics In Japan**. 1: 53-55.

Mogi, K. (1971). Fracture and flow of rocks under high triaxial compression. **Journal Geophysics Reservoir.** 76(5): 1255-1269.

Mogi, K. (1977). Dilatancy of rocks under general triaxial stress states with special reference to earthquake precursors. **Journal of Physics of the Earth Supply**. 25: S203-S217.

Ohokal, M., Funatol, A., and Takahashi, Y. (1997). Tensile test using hollow cylindrical specimen. **International Journal of Rock Mechanics and Mining Sciences**. 34(3-4): 0148-9062.

Oku, H., Haimson, B., and Song, S.R. (2007). True triaxial strength and deformability of the siltstone overlying the Chelungpu fault (Chi-Chi earthquake), Taiwan. **Geophysical Research Letters**. 34(9).

Rao, K.S. and Tiwari, R.P. (2002). Physical simulation of jointed model materials under biaxial and true triaxial stress states. **Research Report, IIT** Delhi, India, pp. 30.

Reddy, K.R., Saxena, S.K., and Budiman, J.S. (1992). Development of a True Triaxial Testing Apparatus. **Geotechnical Testing Journal**. 15(2): 89-105.

Scholz, C.H. (1990). The mechanics of earthquakes and faulting. **Cambridge University Press, U.K.,** pp. 22-23.

Schwab, R. and Benz, T. (2008). A quantitative comparison of six rock failure criteria. **International Journal of Rock Mechanics and Mining Sciences**. 45: 1176-1186.

Sibai, M., Henry, J.P., and Gros, J.C. (1997). Hydraulic fracturing stress measurement using a true triaxial apparatus. **International Journal of Rock Mechanics and Mining Sciences**. 34 (3-4): 289.e1-289.e10.

Singh, B., Goel, R.K., Mehrotra, V.K., Garg, S.K., and Allu, M.R. (1998). Effect of intermediate principal stress on strength of anisotropic rock mass. **Tunneling and Underground Space Technology**. 13: 71-79.

Smart, B.D.G., Somerville J.M., and MacGregor, K.J. (1991). The prediction of yield zone development around a borehole and its effect on drilling and production. **In Rock Mechanics as a Multidisciplinary Science. Proceedings of the 32nd U.S. Symposium on Rock Mechanics,** Norman, Oklahoma., pp. 961-970.

Smart, B.G.D. (1995). A true triaxial cell for testing cylindrical rock specimens. **International Journal of Rock Mechanics and Mining Sciences**. 32(3): 269-275.

Smart, B.D.G., Somerville, J.M., and Crawford, B.R. (1999). A rock test cell with true triaxial capability. **Geotechnical and Geological Engineering, Earth and Environmental Science and Engineering**. 17(3-4): 157-176.

Song, I. and Haimson, B.C. (1997). Polyaxial strength criteria and their use in estimating in situ stress magnitudes from borehole breakout dimensions. **International Journal of Rock Mechanics and Mining Sciences**. 34(3-4): 116.e1-116.e16.

Sture, S. and Desai, C.S. (1979). Fluid cushion truly triaxial or multiaxial testing device. **Geotechnical Testing Journal.** 2: 20-33.

Tepnarong, P. (2001) Theoretical and Experimental Studies to Determine Compressive and Tensile Strength of Rock, Using Modified Point Load Testing. **M.S. Thesis, Suranaree University of Technology,** Thailand.

Tiwari, R.P. and Rao, K.S. (2004). Physical modeling of a rock mass under a true triaxial stress state. **International Journal of Rock Mechanics and Mining Sciences**. 41: 1-6.

Tiwari, R.P. and Rao, K.S. (2006). Post failure behaviour of a rock mass under the influence of triaxial and true triaxial confinement. **Engineering Geology**. 84: 112-129.

Walsri, C., Poonprakon, P., Thosuwan R., and Fuenkajorn, K. (2009). Compressive and tensile strengths of sandstones under true triaxial stresses. In **Proceeding 2nd Thailand Symposium on Rock Mechanics**. Chonburi, Thailand. 2: pp 199-218.

Wang, Q. and Lade, P.V. (2001). Shear banding in true triaxial tests and its effect on failure in sand. **Journal of Engineering Mechanics**. 127: 754-761.

Wawersik, W.R., Carlson, L.W., Holcomb D.J., and Williams, R.J. (1997). New method for true-triaxial rock testing. **International Journal of Rock Mechanics and Mining Sciences and Geomechanics Abstracts**. 34: 365-365.

Wiebols, G.A. and Cook, N.G.W. (1968). An energy criterion for the strength of rock in polyaxial compression. **International Journal of Rock Mechanics and Mining Sciences**. 5: 529-549.

Wijk, G. (1978). Some new theoretical aspects of indirect measurements of tensile strength of rock. **International Journal of Rock Mechanics and Mining Science**s. 15: 149-160.

Worotnicki, G. (1993). CSIRO Triaxial stress measurement cell. **In J.A. Hudson, Editor, Comprehensive Rock Engineering: Principles, Practices, and Projects**. Oxford: Pergamon Press. 6: 169-174.

Yang, X.L., Zou, J.F., and SUI, Z.R. (2007). Effect of intermediate principal stress on rock cavity stability. **Journal Central South University Technology**. s1-0165-05.

You, M. (2008). True-triaxial strength criteria for rock. **International Journal of Rock Mechanics and Mining Sciences**. 46: 115-127.

APPENDIX A

LIST OF PUBLICATIONS

LIST OF PUBLICATIONS

Walsri, C**.,** Poonprakon, P**.,** Thosuwan R. and Fuenkajorn, K., 2009. **Compressive and tensile strengths of sandstones under true triaxial stresses**. In Proceedings 2nd Thailand Symposium on Rock Mechanics. Chonburi, Thailand. 12 - 13 March 2009.

Thosuwan R., Walsri, C., Poonprakon, P**.** and Fuenkajorn, K., 2009. **Effects of intermediate principal on compressive and tensile strengths of sandstones**. In International Symposium on Rock Mechanics "Rock Characterization, Modelling, and Engineering Design Methods. University of Hong Kong, Hong Kong. 19-22 May 2009.

Rock Mechanics, Fuenkajorn & Phien-wej (eds) © 2009. ISBN 978 974 533 624 7

Compressive and tensile strengths of sandstones under true triaxial stresses

C. Walsri, P. Poonprakon, R. Thosuwan & K. Fuenkajorn
Geomechanics Research Unit, Suranaree University of Technology, Thailand

Keywords: True triaxial, polyaxial, intermediate principal stress, sandstone, anisotropic

ABSTRACT: A polyaxial load frame has been developed to determine the compressive and tensile strengths of three types of sandstone under true triaxial stresses. Results from the polyaxial compression tests on rectangular specimens of sandstones suggest that the rocks are transversely isotropic. The measured elastic modulus in the direction parallel to the bedding planes is slightly greater than that normal to the bedding. Poisson's ratio on the plane normal to the bedding planes is lower than those on the parallel ones. Under the same σ_3, σ_1 at failure increases with σ_2. Results from the Brazilian tension tests under axial compression reveal the effects of the intermediate principal stress on the rock tensile strength. The Coulomb and modified Wiebols and Cook failure criteria derived from the characterization test results predict the sandstone strengths in term of $J_2^{1/2}$ as a function of J_1 under true triaxial stresses. The modified Wiebols and Cook criterion describes the failure stresses better than does the Coulomb criterion when all principal stresses are in compressions. When the minimum principal stresses are in tension, the Coulomb criterion over-estimate the second order of the stress invariant at failure by about 20% while the modified Wiebols and Cook criterion fails to describe the rock tensile strengths.

1 INTRODUCTION

The effects of confining pressures at great depths on the mechanical properties of rocks are commonly simulated in a laboratory by performing triaxial compression testing of cylindrical rock core specimens. A significant limitation of these conventional methods is that the intermediate and minimum principal stresses are equal during the test while the actual in-situ rock is normally subjected to an anisotropic stress state where the maximum, intermediate and minimum principal stresses are different ($\sigma_1 \neq \sigma_2 \neq \sigma_3$). It has been commonly found that compressive strengths obtained from conventional triaxial testing can not represent the actual in-situ strength where the rock is subjected to an anisotropic stress state (Yang et al., 2007; Haimson, 2006; Tiwari & Rao, 2004, 2006; Haimson & Chang, 1999). A variety of devices have been developed for rock testing under true triaxial stresses. Some recent ones include those proposed by Reddy et al. (1992), Smart (1995), Wawersik et al. (1997), Haimson & Chang (2000), and Alexeev et al. (2004). These devices are mostly designed for testing rock specimens under compression.

From the experimental results on brittle rocks obtained by the researchers above (e.g., Colmenares & Zoback, 2002; Haimson, 2006) it can be generally concluded that in a σ_1 - σ_2 diagram, for a given σ_3, σ_1 at failure initially increases with σ_2 to a certain magnitude, and then it gradually decreases as σ_2 increases. The effect of σ_2 is more pronounced under higher σ_3. Cai (2008) offers an explanation of how the intermediate principal stress affects the rock strength based on the results from numerical simulations on fracture initiation and propagation. He states that the intermediate principal stress confines the rock in such a way that fractures can only be initiated and propagated in the direction parallel to σ_1 and σ_2. The effect of σ_2 is related to the stress-induced anisotropic properties and behavior of the rock and to the end effect at the interface between the rock surface and loading platen in the direction of σ_2 application. The effect should be smaller in homogeneous and fine-grained rocks than in coarse-grained rocks where pre-existing micro-cracks are not uniformly distributed.

Several failure criteria have been developed to describe the rock strength under true triaxial stress states. Comprehensive reviews of these criteria have been given recently by Colmenares & Zoback (2002), Al-Ajmi & Zimmerman (2005), Haimson (2006), Benz & Schwab (2008), Cai (2008), Haimson & Hudson (2008) and You (2008). Among several other criteria, the Mogi and modified Wiebols and Cook criteria are perhaps the most widely used to describe the rock compressive strengths under true triaxial stresses. These strength criteria however have rarely been verified when one or two of the principal stresses are in tension. Obtaining rock strengths under an anisotropic stress state is not only difficult but expensive. A special loading device (e.g., polyaxial loading machine or true triaxial load cell) is required. As a result test data under true triaxial stress conditions have been relatively limited. Most researchers above have used the same sets of test data (some obtained over a decade ago) to compare with their new numerical simulations, field observations (notably on breakout of deep boreholes) or to verify their new strength criteria and concepts. Due to the cost and equipment availability for obtaining true triaxial strengths, in common engineering practices application of a failure criterion that can incorporate the three-dimensional stresses has been very rare.

This research involves the development of a simple and low-cost polyaxial load frame to test rock specimens under true triaxial stress states. The frame performance is assessed by conducting polyaxial compression tests and Brazilian tension tests under axial compression to study the deformation and failure characteristics of sandstone specimens. The Coulomb and modified Wiebols and Cook failure criteria derived from the results of conventional tests are used to describe the compressive and tensile strengths of the rocks under true triaxial stress states.

2 ROCK SAMPLES

The tested sandstones are from three sources: Phu Phan, Phra Wihan and Phu Kradung formations (hereafter designated as PP, PW and PK sandstones). These fine-grained quartz sandstones are selected primarily because of their highly uniform texture, density and strength. Their average grain size is 0.1-1.0 mm. They are commonly found in the north and northeast of Thailand. Their mechanical properties and responses play a significant role in the stability of tunnels, slope embankments and dam foundations in the region. For the polyaxial compression testing rectangular block specimens are cut and ground to have a nominal dimension of 5×5×10 cm. The perpendicularity and parallelism of the specimens follow the ASTM (D 4543) specifications. The longest axis is parallel to the bedding planes and to the direction of the major principal stress. Though having different shape the

Rock Mechanics, Fuenkajorn & Phien-wej (eds) © 2009. ISBN 978 974 533 624 7

specimens used here have volume and length-to-diameter ratio comparable to those used in the conventional uniaxial and triaxial compression test methods. The Brazilian tension test uses disk specimens with a nominal diameter of 50 mm with a thickness-to-diameter ratio of 0.5 to comply with ASTM D 3967-95. The core axis is normal to the bedding planes. All specimens are oven-dried before testing.

3 POLYAXIAL LOAD FRAME

The development of the polyaxial load frame is based on three key design requirements: (1) capable of maintaining constant lateral stresses (σ_2 and σ_3) during the test, (2) capable of testing specimen with volume equal to or larger than those used in the conventional triaxial testing, and (3) allowing monitoring of specimen deformation along the principal axes. Figure 1 shows the polyaxial load frame developed in this research. To meet the load requirement above, two pairs of cantilever beams are used to apply the lateral stresses in mutually perpendicular directions to the rock specimen. The outer end of each opposite beam is pulled down by dead weight placed in the middle of a steel bar linking the two opposite beams underneath (Figure 2). The inner end is hinged by a pin mounted on vertical bars on each side of the frame. During testing all beams are arranged perfectly horizontally, and hence a lateral compressive load results on the specimen placed at the center of the frame. Due to the different distances from the pin to the outer weighting point and from the pin to the inner loading point, a load magnification of 17 to 1 is obtained from load calibration with an electronic load cell. This loading ratio is also used to determine the lateral deformation of the specimen by monitoring the vertical movement of the two steel bars below. The maximum lateral load is designed for 100 kN. The axial load is applied by a 1000-kN hydraulic load cell. The load frame can accommodate specimen sizes from 2.5×2.5×2.5 cm to 10×10×20 cm. The different specimen sizes and shapes can be tested by adjusting the distances between the opposite loading platens. Note that virtually all true triaxial and polyaxial cells previously developed elsewhere can test rock samples with the maximum size not larger than 5×5×10 cm.

4 POLYAXIAL COMPRESSION TESTS

The polyaxial compression tests are performed to determine the compressive strengths and deformations of the PK, PP and PW sandstones under true triaxial stresses. The intermediate (σ_2) and minimum (σ_3) principal stresses are maintained constant while σ_1 is increased until failure. Here the constant σ_2 is varied from 0 to 17 MPa, and σ_3 from 0 to 6 MPa. Neoprene sheets are used to minimize the friction at all interfaces between the loading platen and the rock surface. Figure 3 shows the applied principal stress directions with respect to the bedding planes for all specimens. The measured sample deformations are used to determine the strains along the principal axes during loading. The failure stresses are recorded and mode of failure examined.

4.1 Test Results

Figure 4 plots the stress-strain curves from the start of loading to failure for some sandstone specimens. The elastic modulus and Poisson's ratio are calculated for the directions normal and parallel to the bedding planes. Under the stress orientation used here where σ_1 and σ_2 are parallel to the bedding planes, the three-dimensional principal stress-strain relations given by Jaeger & Cook (1979) can be simplified to obtain a set of governing equations for a transversely isotropic material as:

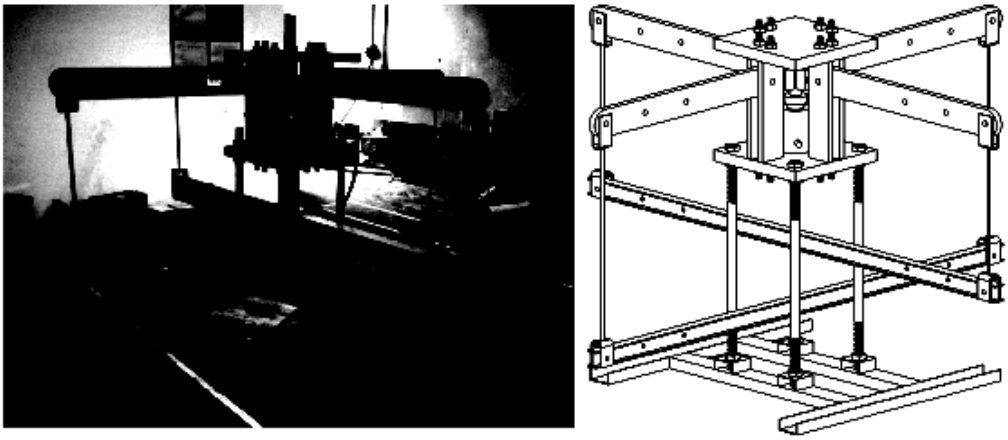

Figure 1. Polyaxial load frame developed for compressive and tensile strength testing under true triaxial stress.

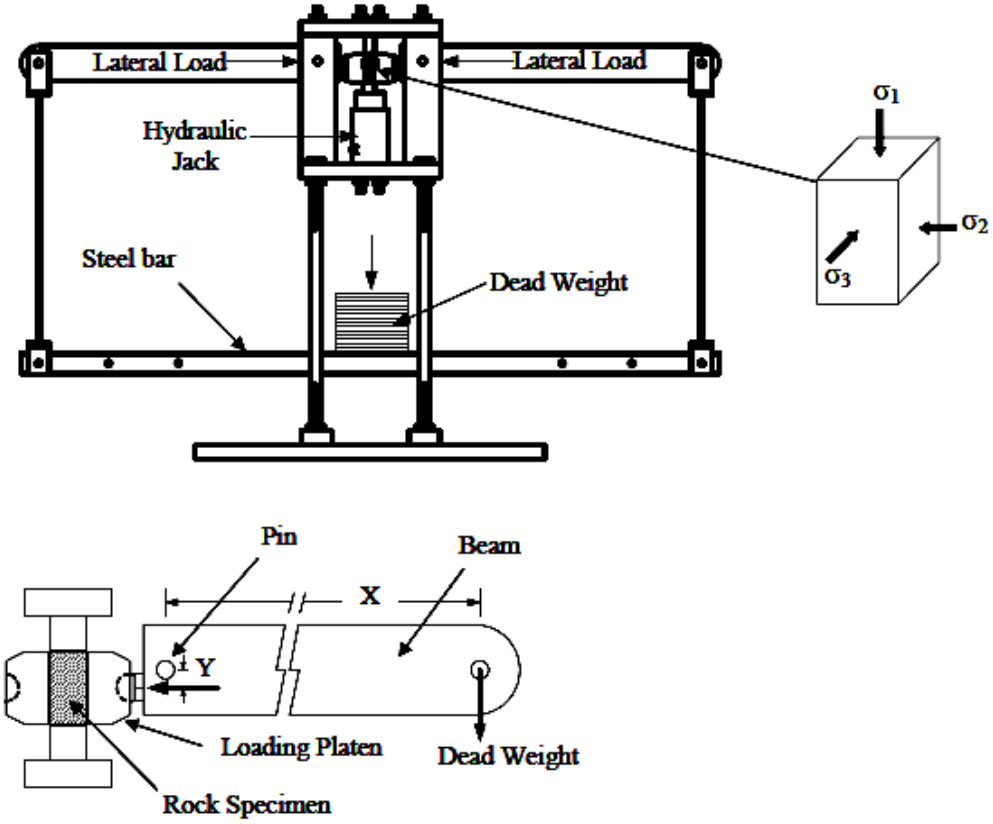

Figure 2. Cantilever beam weighed at outer end applies lateral stress to the rock specimen.

Rock Mechanics, Fuenkajorn & Phien-wej (eds) © 2009. ISBN 978 974 533 624 7

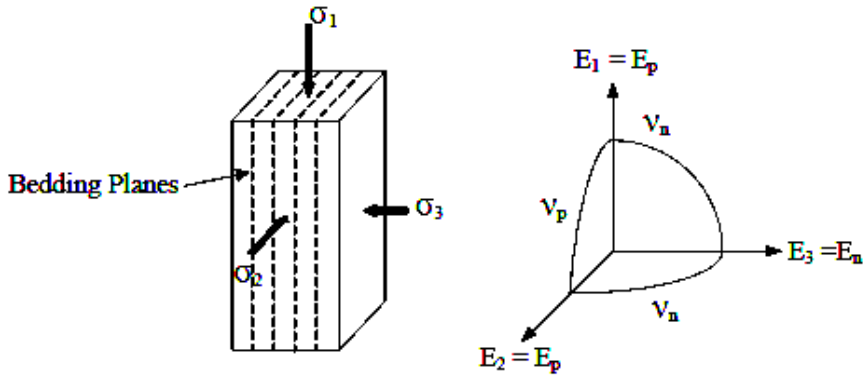

Figure 3. Directions of loading with respect to the bedding planes (left). Elastic parameters for transversely isotropic conditions (right).

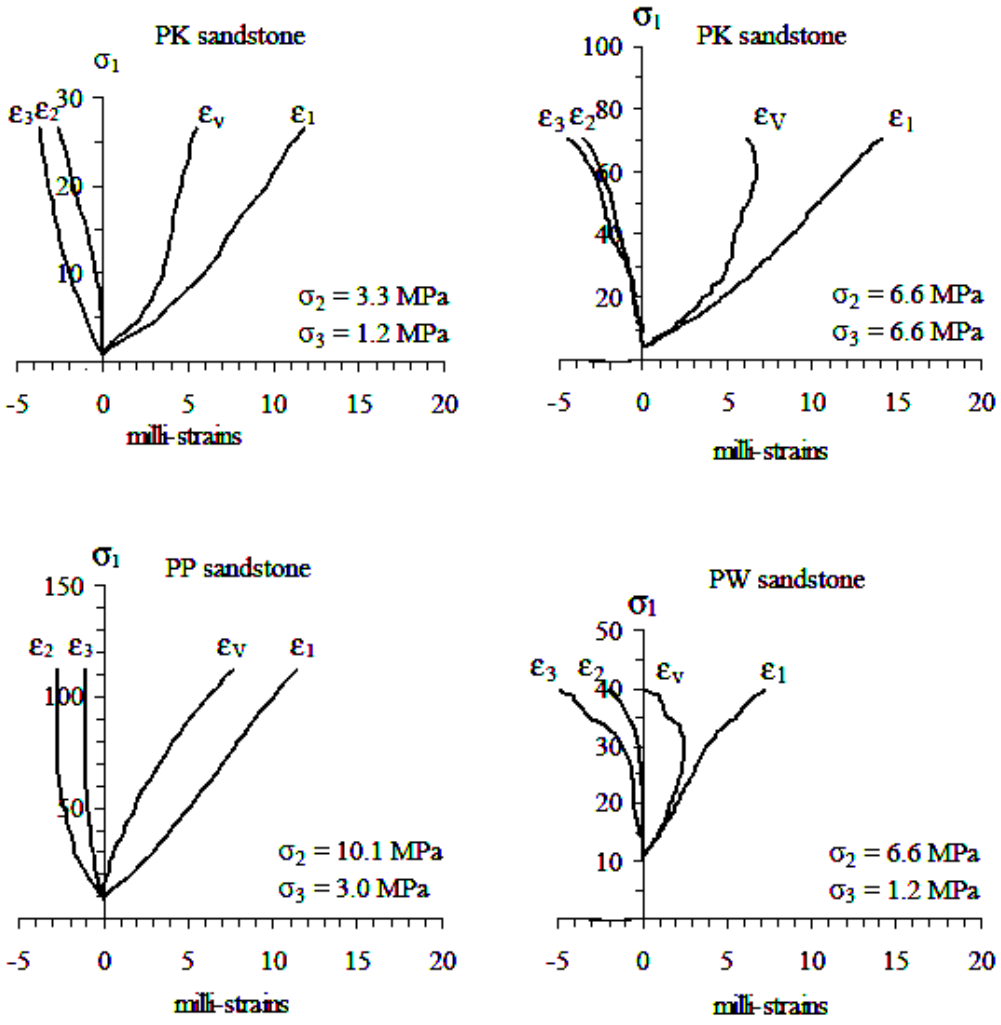

Figure 4. Examples of stress-strain curves of the three sandstones under polyaxial loading.

$$\varepsilon_1 = \frac{\sigma_1}{E_p} - \frac{\sigma_2 \nu_p}{E_p} - \frac{\sigma_3 \nu_n}{E_n} \quad (1)$$

$$\varepsilon_2 = -\frac{\sigma_1 \nu_p}{E_p} + \frac{\sigma_2}{E_p} - \frac{\sigma_3 \nu_n}{E_n} \quad (2)$$

$$\varepsilon_3 = -\frac{\sigma_1 \nu_n}{E_p} - \frac{\sigma_2 \nu_n}{E_p} + \frac{\sigma_3}{E_n} \quad (3)$$

where: σ_1, σ_2 and σ_3 are principal stresses, ε_1, ε_2 and ε_3 are principal strains, E_n and E_p are elastic moduli normal and parallel to the bedding planes, and ν_n and ν_p are Poisson's ratio's on the planes normal and parallel to the bedding.

The calculations of the Poisson's ratios and tangent elastic moduli are made at 50% of the maximum principal stress. The PW and PP sandstones exhibit a small transversely isotropic behavior. The elastic modulus in the direction normal to the bedding planes is slightly lower than that parallel to the bedding planes. The Poisson's ratio on the plane parallel to the beds is less than that across the beds. Table 1 summarizes the elastic parameters with respect to the bedding plane orientation.

Figure 5 plots σ_1 at failure as a function of σ_2 tested under various σ_3's for the PW and PP sandstones. The results show the effects of the intermediate principal stress, σ_2, on the maximum stresses at failure by the failure envelopes being offset from the condition where $\sigma_2 = \sigma_3$. For all minimum principal stress levels, σ_1 at failure increases with σ_2. The effect of σ_2 tends to be more pronounced under a greater σ_3. These observations agree with those obtained elsewhere (e.g. Haimson & Chang, 2000; Colmenares & Zoback, 2002; Haimson, 2006). Post-failure observations suggest that compressive shear failures are predominant in the specimens tested under low σ_2 while splitting tensile fractures parallel to σ_1 and σ_2 directions dominate under higher σ_2 (Figure 6). The observed splitting tensile fractures under relatively high σ_2 suggest that the fracture initiation has no influence from the friction at the loading interface in the σ_2 direction. As a result the increase of σ_1 with σ_2 should not be due to the interface friction. This does not agree with a conclusion drawn by Cai (2008) that friction at the interface in the σ_2 direction contributes to the increase of σ_1 at failure. Under the conditions when $\sigma_2 = \sigma_3$, the magnitudes of σ_1 at failure agree well with the triaxial compressive strength test results obtained by Kenkhunthod and Fuenkajorn (2009).

4.2 Strength Criteria

The Coulomb and modified Wiebols and Cook failure criteria are used to describe the polyaxial strengths of the PW and PP sandstones. They are selected because the Coulomb criterion has been widely used in actual field applications while the modified Wiebols and Cook criterion has been claimed by many researchers to be one of the best representations of rock strengths under polyaxial compression. To represent the rock strengths under true triaxial stresses the second order stress invariant ($J_2^{1/2}$) and the first order stress invariant or the mean stress (J_1) are calculated from the test results by the following relations (Jaeger & Cook, 1979):

$$J_2^{1/2} = \sqrt{(1/6)\{(\sigma_1 - \sigma_2)^2 + (\sigma_1 - \sigma_3)^2 + (\sigma_2 - \sigma_3)^2\}} \quad (4)$$

Rock Mechanics, Fuenkajorn & Phien-wej (eds) © 2009. ISBN 978 974 533 624 7

Table 1. Elastic properties in the direction normal and parallel to bedding planes.

	Rock Types	E_p (GPa)	E_n (GPa)	ν_p	ν_n
Polyaxial Compression Test	PW	10.0	8.6	0.38	0.28
	PP	11.1	10.3	0.36	0.33
Brazilian Tension Test	PW	9.2	N/A	0.21	N/A
	PP	14.8	N/A	0.19	N/A
	PK	5.9	N/A	0.11	N/A

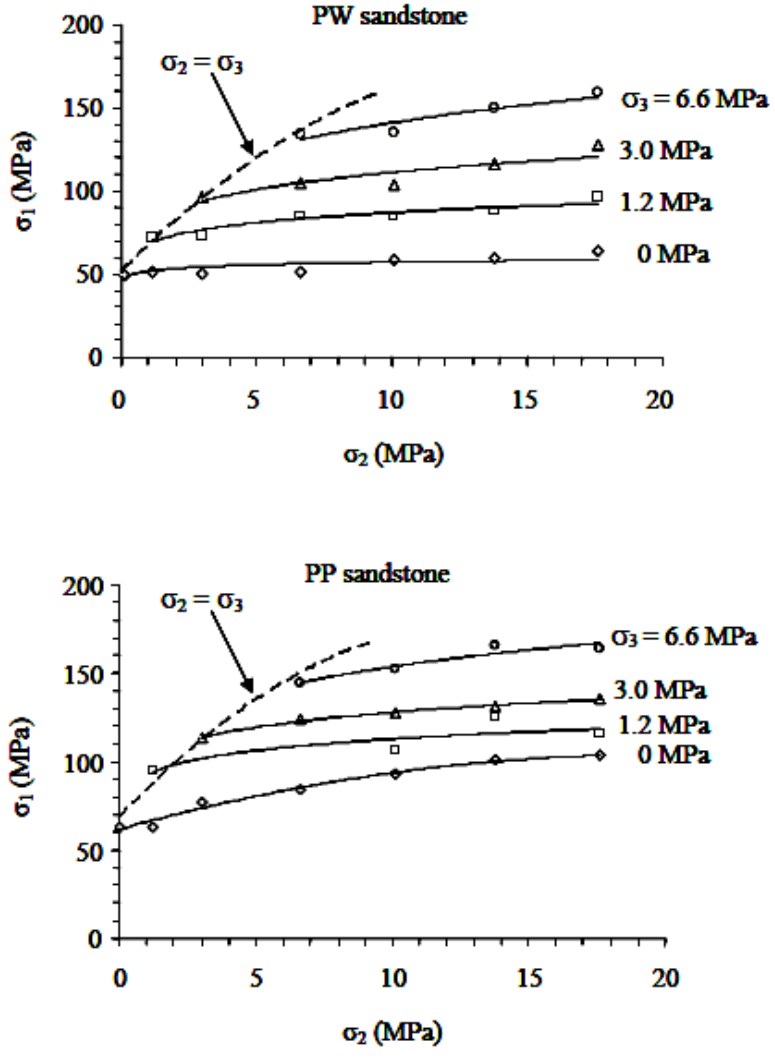

Figure 5. Maximum principal stress (σ_1) at failure as a function of σ_2 for various σ_3 values.

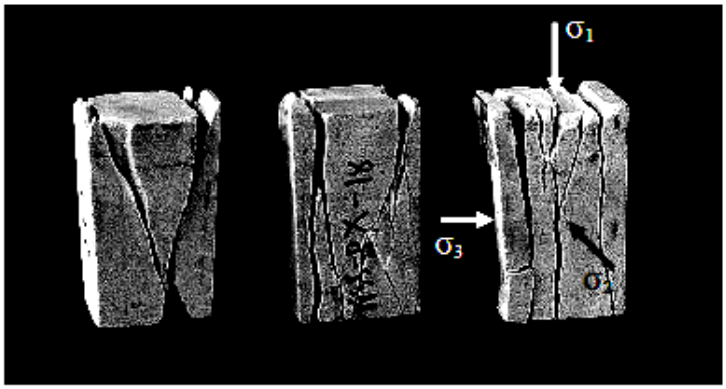

Figure 6. Post-tested specimens of PW sandstone. Left: $\sigma_1 = 51$, $\sigma_2 = 1.2$, $\sigma_3 = 0$ MPa. Middle: $\sigma_1 = 50$, $\sigma_2 = 3.0$, $\sigma_3 = 0$ MPa. Right: $\sigma_1 = 58.8$, $\sigma_2 = 10.0$, $\sigma_3 = 0$ MPa.

$$J_1 = (\sigma_1 + \sigma_2 + \sigma_3)/3 \tag{5}$$

Here the Coulomb criterion is derived from the uniaxial and triaxial compressive strengths of the rocks where σ_2 and σ_3 are equal. Figures 7 and 8 compare the polyaxial test results with those predicted by the Coulomb criterion for PW and PP sandstones. The predictions are made for σ_3 = 0, 1.2, 3.0 and 6.6 MPa (as used in the tests) and under stress conditions from $\sigma_2 = \sigma_3$ to $\sigma_1 = \sigma_2$. In the $J_2^{1/2}$ - J_1 diagram, $J_2^{1/2}$ increases with σ_3 but it is independent of J_1 because the Coulomb criterion ignores σ_2 in the strength calculation. Under a low σ_2 and σ_3 the Coulomb prediction tends to agree with the test results obtained from the PW sandstone. Except for this case, no correlation between the Coulomb predictions and the polyaxial strengths can be found. The inadequacy of the predictability of Coulomb criterion under polyaxial stress states obtained here agrees with a conclusion drawn by Colmenares & Zoback (2002).

The modified Wiebols and Cook criterion given by Colmenares & Zoback (2002) defines $J_2^{1/2}$ at failure in terms of J_1 as:

$$J_2^{1/2} = A + BJ_1 + CJ_1^2 \tag{6}$$

The constants A, B and C depend on rock materials and the minimum principal stresses (σ_3). They can be determined under the conditions where $\sigma_2 = \sigma_3$, as follows (Colmenares & Zoback, 2002):

$$C = \frac{\sqrt{27}}{2C_1 + (q-1)\sigma_3 - C_0} \times \left(\frac{C_1 + (q-1)\sigma_3 - C_0}{2C_1 + (2q+1)\sigma_3 - C_0} - \frac{q-1}{q+2} \right) \tag{7}$$

where: $C_1 = (1 + 0.6\mu_i)C_0$ (8)

C_0 = uniaxial compressive strength of the rock.

$\mu_i = \tan\phi$ (9)

$q = \{(\mu_i^2 + 1)^{1/2} + \mu_i\}^2 = \tan^2(\pi/4 + \phi/2)$ (10)

$$B = \frac{\sqrt{3}(q-1)}{q+2} - \frac{C}{3}(2C_0 + (q+2)\sigma_3 \tag{11}$$

Rock Mechanics, Fuenkajorn & Phien-wej (eds) © 2009. ISBN 978 974 533 624 7

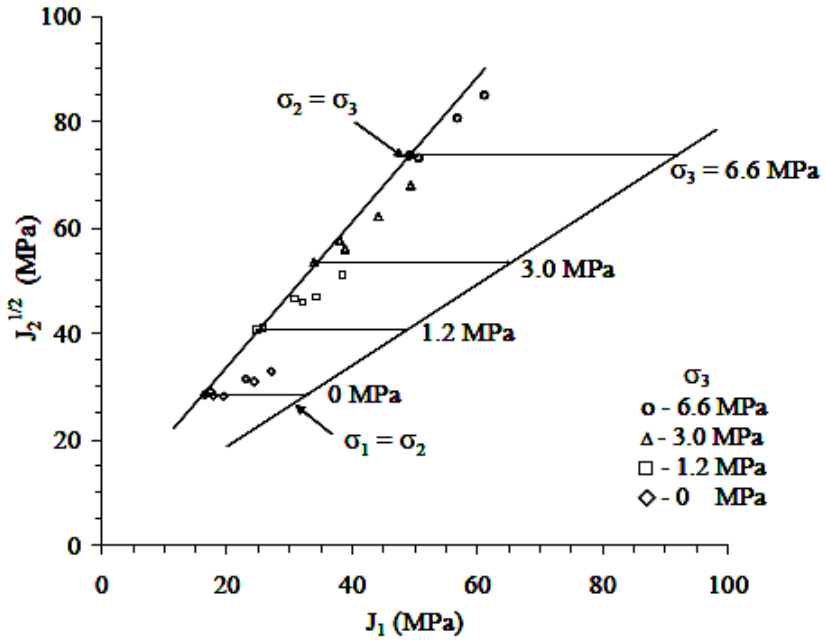

Figure 7. $J_2^{1/2}$ as a function of J_1 from testing PW sandstone compared with the Coulomb criterion predictions (lines).

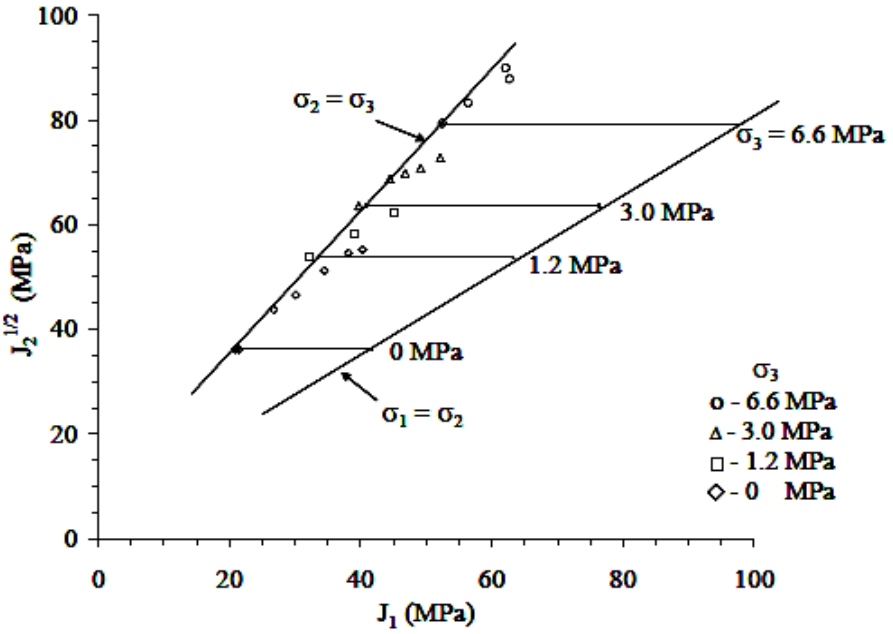

Figure 8. $J_2^{1/2}$ as a function of J_1 from testing PP sandstone compared with the Coulomb criterion predictions (lines).

$$A = \frac{C_0}{\sqrt{3}} - \frac{C_0}{3}B - \frac{{C_0}^2}{9}C \qquad (12)$$

The numerical values for A, B and C for PW and PP sandstones are given in Table 2 for each σ_3 tested here. Substituting these constants into equation (6), the upper and lower limits of $J_2^{1/2}$ for each rock type can be defined under conditions of $\sigma_2 = \sigma_3$ and $\sigma_1 = \sigma_2$. The predictions are made for σ_3 = 0, 1.2, 3.0 and 6.6 MPa. Figures 9 and 10 compare the test results with those predicted by the modified Wiebols and Cook criterion. The predictions tend to be higher than the sandstone strengths under low σ_3. Under a higher σ_3 the criterion well represents the polyaxial strengths of the rocks. This conforms to the results obtained by Colmenares & Zoback (2002) that predictive capability of the modified Wiebols and Cook criterion improves as the minimum principal stress increases.

5 BRAZILIAN TENSION TESTS UNDER AXIAL COMPRESSION

The Brazilian tension tests with axial compression have been performed on PP, PW and PK sandstone disks to determine the effects of the intermediate principal stress on the rock tensile strength. The polyaxial load frame is used to apply a constant axial stress on the disk specimen while the diametral line load is increased until failure (Figure 11). The constant axial stress is varied from zero (Brazilian test) to as high as the rock compressive strength. Neoprene sheets are used to minimize the friction between the rock surface and loading platen in the axial direction.

5.1 Brazilian Tension Test Results

Figure 12 plots the line load at failure (P_f) as a function of the axial stress (σ_z) for the three sandstones. The failure load linearly decreases with increasing axial stress. At $P_f = 0$ the axial stress becomes the uniaxial compressive strength of the rock. The tensile stresses (σ_x) and compressive stresses (σ_y) induced at the crack initiation point in the middle of the specimen also decrease with increasing axial stress (Figure 13). These stresses are calculated from the solutions given by Jaeger & Cook (1979). The test results reveal a linear transition from the Brazilian tensile strength to the uniaxial compressive strength, which can be best demonstrated by using Mohr's circles, as shown in Figure 14.

Post-failure observations show that under low σ_z a single splitting extension crack along the loading diameter is normally induced in the disk specimen. Multiple extension cracks are developed as σ_z increase. When σ_z reaches the uniaxial compressive strength of the rocks, the specimens fail without applying the diametral line load. At this point the specimens are crushed, resulting in multiple shear fractures and extension cracks (Figure 15). It is postulated that the axial stress produces tensile strains perpendicular to its direction due to the effect of the Poisson's ratio. At the crack initiation point this tensile strain is combined with

Table 2. Parameters A, B and C for PW and PP sandstones.

Rock types	PW Sandstone				PP Sandstone			
σ_3 (MPa)	0	1.2	3.0	6.6	0	1.2	3.0	6.6
A (MPa)	1.37	0.54	-0.41	-1.7	1.97	1.16	0.17	-1.2
B	1.92	1.94	1.96	1.99	1.91	1.92	1.94	1.96
C (MPa^{-1})	-0.016	-0.014	-0.012	-0.009	-0.013	-0.013	-0.01	-0.008

Rock Mechanics, Fuenkajorn & Phien-wej (eds) © 2009. ISBN 978 974 533 624 7

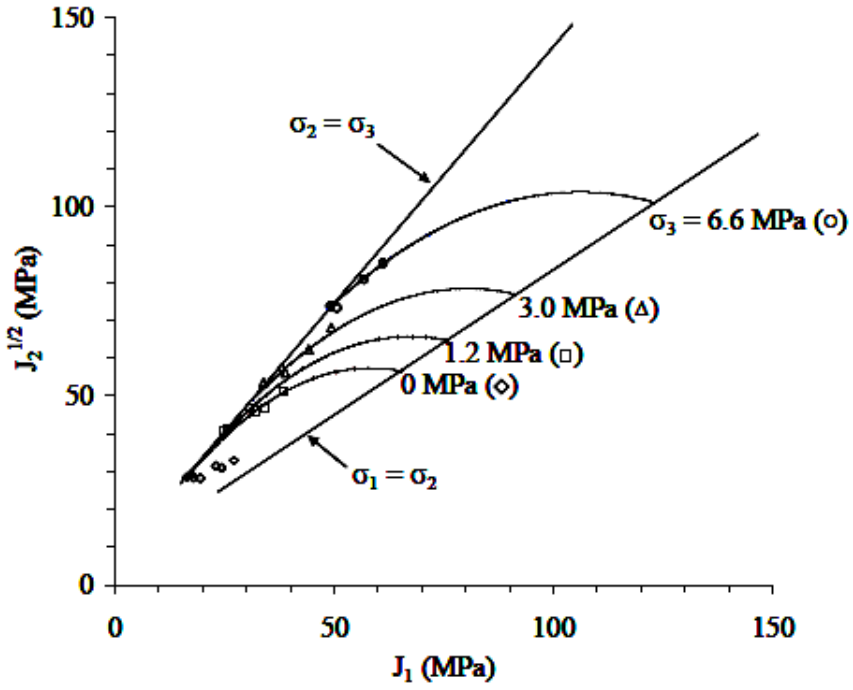

Figure 9. $J_2^{1/2}$ as a function of J_1 from testing PW sandstone compared with the modified Wiebols and Cook criterion predictions (lines).

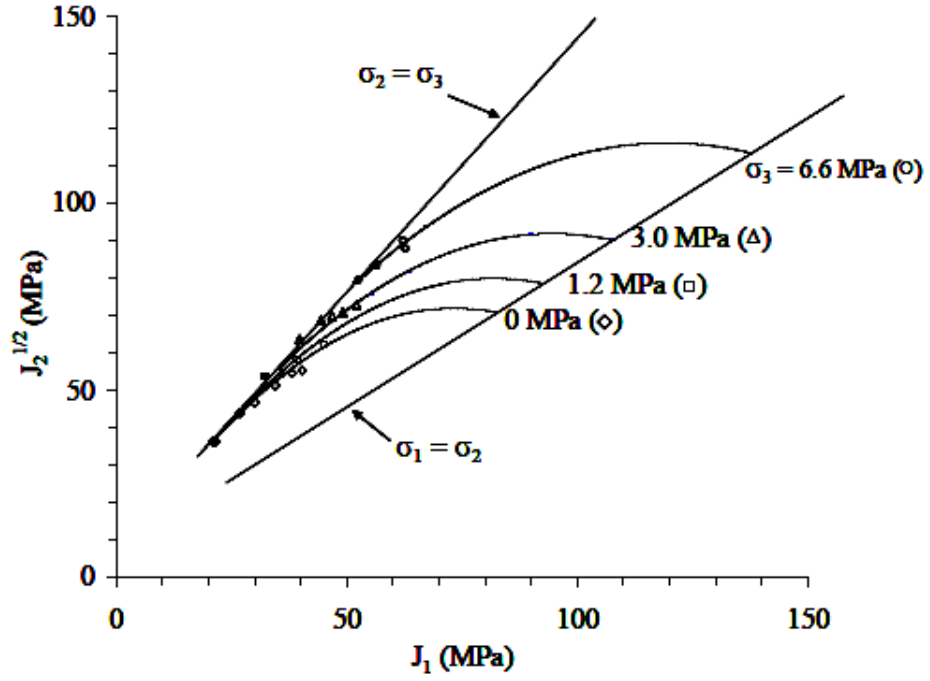

Figure 10. $J_2^{1/2}$ as a function of J_1 from testing PP sandstone compared with the modified Wiebols and Cook criterion predictions (lines).

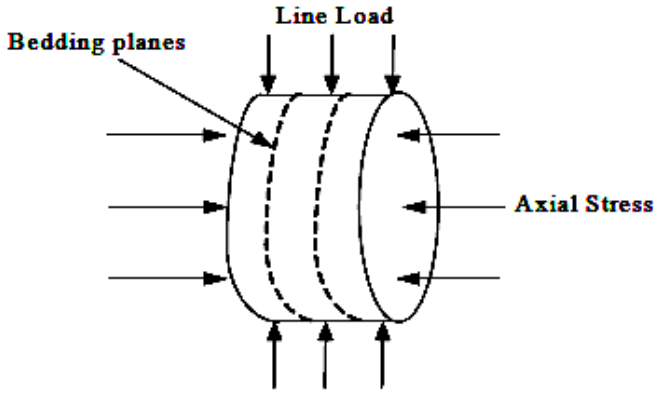

Figure 11. Brazilian tension test specimen under axial compression.

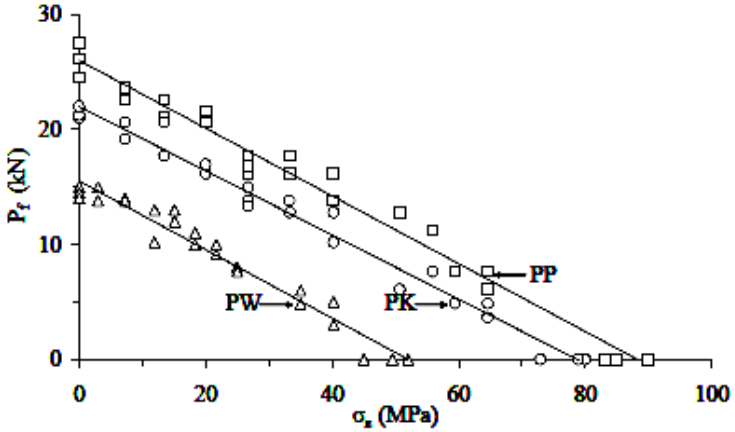

Figure 12. Line load at failure (P_f) as a function of applied axial stress (σ_z).

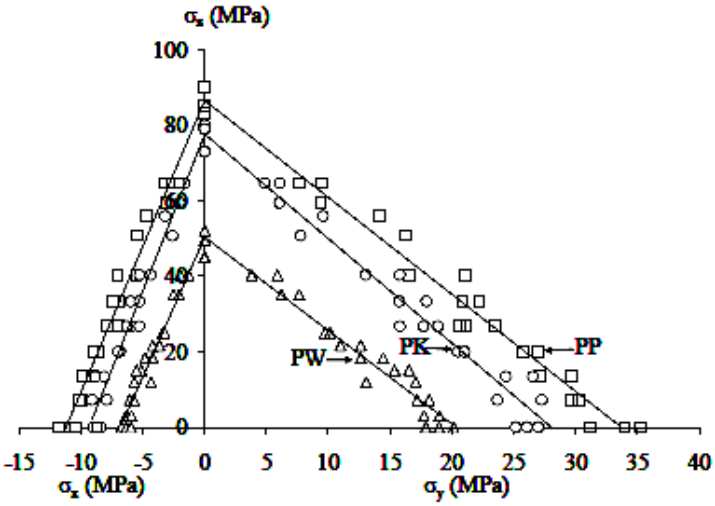

Figure 13. Induced compressive (σ_y) and tensile stresses (σ_x) at failure as a function of applied σ_z.

Rock Mechanics, Fuenkajorn & Phien-wej (eds) © 2009. ISBN 978 974 533 624 7

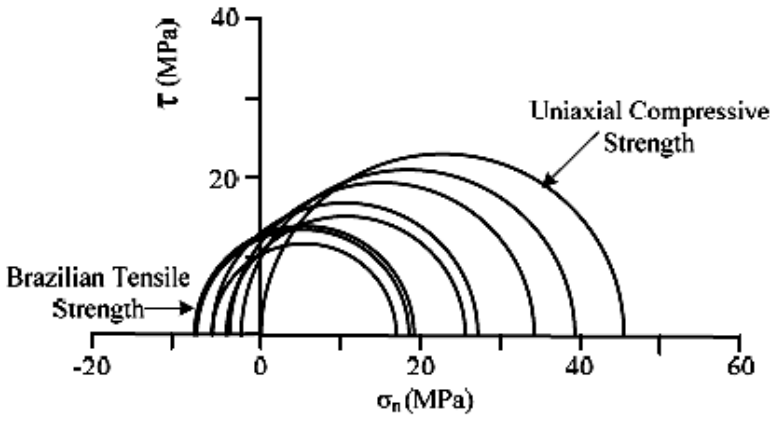

Figure 14. Mohr's circles from testing of PW sandstone showing transition from Brazilian tensile strength to uniaxial compressive strength.

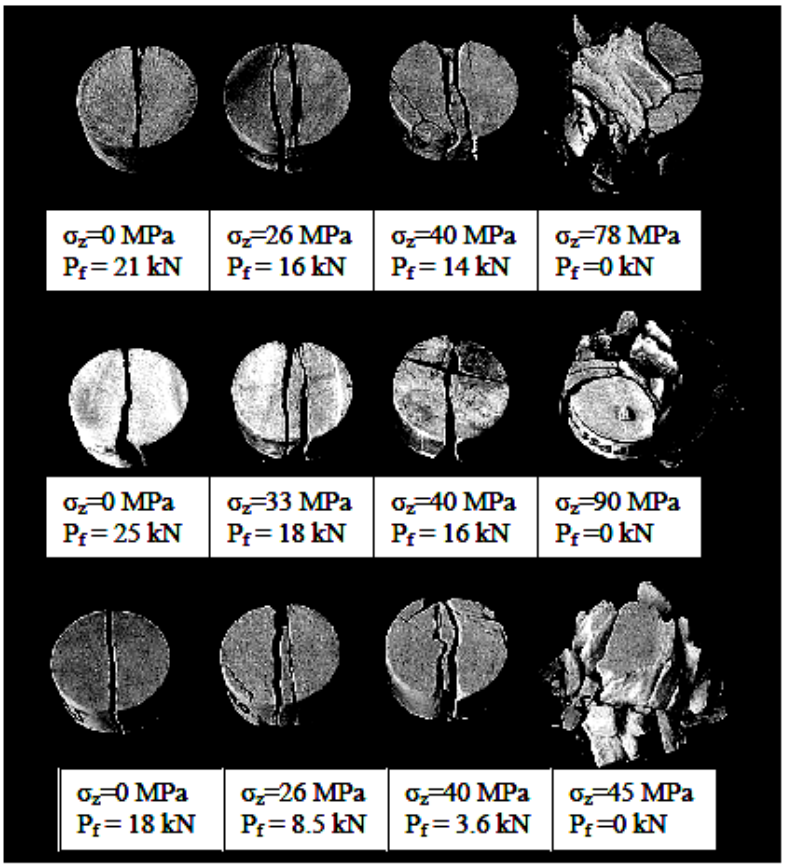

Figure 15. Some post- test specimens of PK sandstone (top), PP sandstone (middle) and PW sandstone (bottom).

the horizontal tensile stress that is induced by the line load. The line load at failure therefore decreases with increasing σ_z. Calculation of the σ_z-induced tensile strain for the entire specimen is however not that simple because the rock is under both tension and compression and the elastic properties under tension and compression may be different (Jaeger & Cook, 1979; Chen et al., 1998). More discussion on this issue is given in the next section.

Under no axial stress the elastic modulus and Poisson's ratio of the sandstones are measured by installing strain gages at the center of the sandstone specimen. The gages measure the vertical compressive strain, ε_y, (along the loading diameter) and horizontal tensile strain, ε_x, induced during line loading. Three samples have been tested for each rock type. Figure 16 plots the measured strains as a function of the applied load, P. The elastic modulus and Poisson's ratio can be calculated using the following equations (Hondros, 1959):

$$\nu = -\frac{3\varepsilon_x + \varepsilon_y}{3\varepsilon_y + \varepsilon_x} \tag{13}$$

$$E = \frac{2P(1-\nu)^2}{\pi Dt(\varepsilon_x + \nu\varepsilon_y)} \tag{14}$$

These equations assume that the rock is linearly elastic and isotropic and that the elastic modulus in tension is equal to that in compression. The E and ν above are compared with those obtained from the polyaxial compression testing in Table 1. Since all Brazilian disks are prepared to have bedding planes normal to the disk axis, only elastic modulus and Poisson's ratio parallel to the bedding can be measured. The discrepancy of the elastic parameters obtained from the two test types may be because the rock elastic modulus under tension is lower than that under compression and there is intrinsic variability among the tested specimens.

5.2 Strength Criteria under Tension

The Coulomb and modified Wiebols and Cook failure criteria are used to describe the rock strengths when the minimum principal stress is in tension. First the results of the Brazilian tests under axial compression are calculated in terms of $J_2^{1/2}$ as a function of J_1. The induced horizontal tensile stress (σ_x) always represents the minimum principal stress (σ_3) in this test. Under low axial stress, the vertical compressive stress (σ_y) at the crack initiation point represents the maximum principal stress (σ_1), and the axial stress represents the intermediate principal stress (σ_2). When the axial stress is increased beyond a certain magnitude, σ_z becomes σ_1, and σ_y becomes σ_2.

From the test results the stress invariant $J_2^{1/2}$ as a function of mean stress J_1 is compared with the predictions by the Coulomb criterion in Figure 17 for PP, PW and PK sandstones. Since the Coulomb criterion ignores σ_2 at failure, the predicted $J_2^{1/2}$ is independent of J_1 for each σ_3. The predicted $J_2^{1/2}$ decreases with σ_3 when the applied axial stress (σ_z) represents σ_1, and increases with σ_3 when the induced vertical stress (σ_y) represents σ_1. These stress variations conform well to the actual test results. The Coulomb criterion over-estimates the actual strengths for all levels of σ_3. On average the discrepancies are about 15-20%.

Rock Mechanics, Fuenkajorn & Phien-wej (eds) © 2009. ISBN 978 974 533 624 7

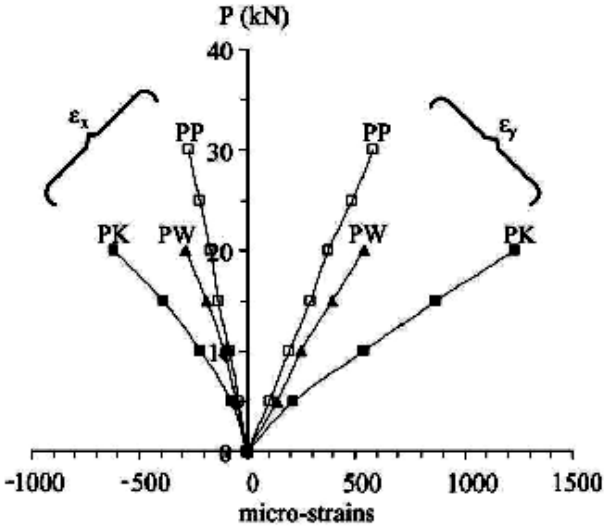

Figure 16. Strain measurements from Brazilian testing on PP, PW and PK sandstones.

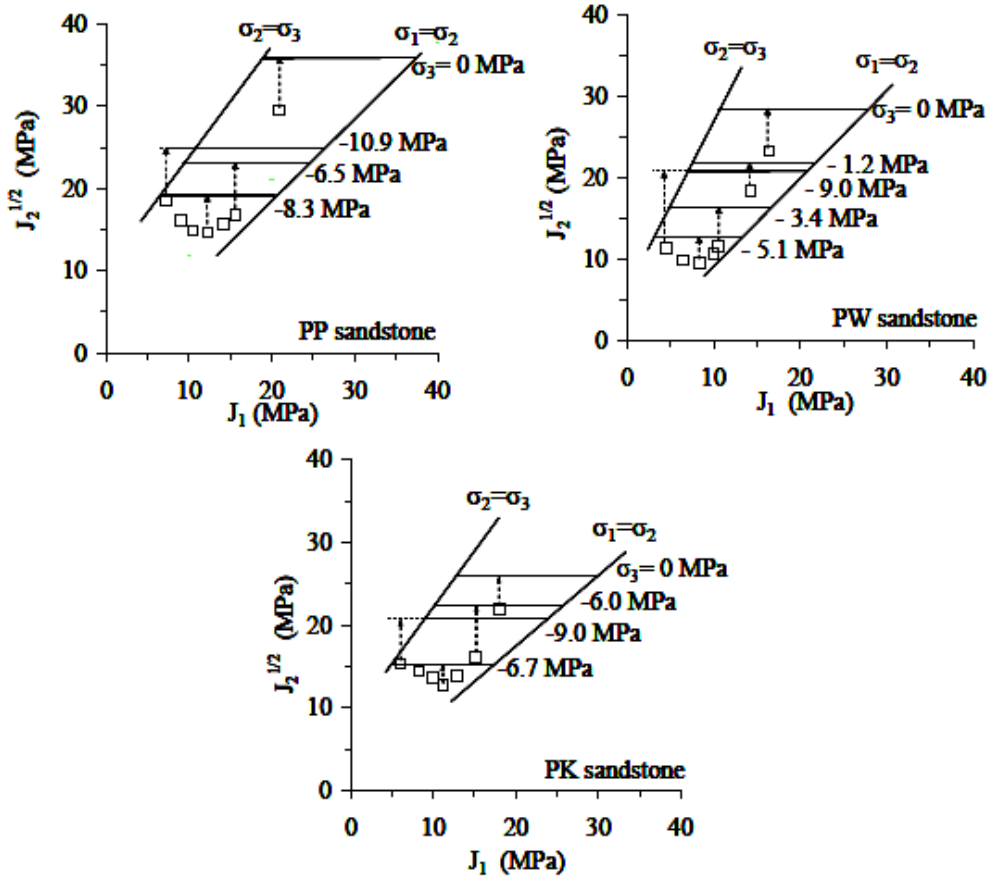

Figure 17. $J_2^{1/2}$ as a function of J_1 for Brazilian testing on PP, PW and PK sandstones compared with the Coulomb criterion predictions.

Figure 18 compares the measured strengths with the predictions by the modified Wiebols and Cook criterion for the three sandstones. The criterion is not sensitive to the observed variations of the rock strengths in the $J_2^{1/2}$ - J_1 diagram. The predicted $J_2^{1/2}$ curves continue to decrease as the minimum stress decreases. This does not strictly reflect the actual observations where $J_2^{1/2}$ increases after the induced vertical stress becomes the maximum principal stress. It appears that the modified Wiebols and Cook criterion can not describe the rock strengths when the minimum principal stress is in tension.

7 DISSCUSSIONS AND CONCLUSIONS

The invented polyaxial load frame performs well for the assessment of the effects of σ_2 on the compressive and tensile strengths of the sandstones. Measuring the specimen deformations by monitoring the movement of the cantilever beams is sufficiently accurate and sensitive to detect the transversely isotropic behavior of the PW and PP sandstones. An advantage of the polyaxial frame is that it can test rock specimens with a wider range of sizes and shapes as compared to most true triaxial cells previously developed. Such flexibility allows us to perform a variety of test configurations, for example polyaxial creep testing, four-point beam bending tests with lateral confinement, Brazilian and ring tension tests with axial compression, and borehole stability testing under biaxial and polyaxial stresses.

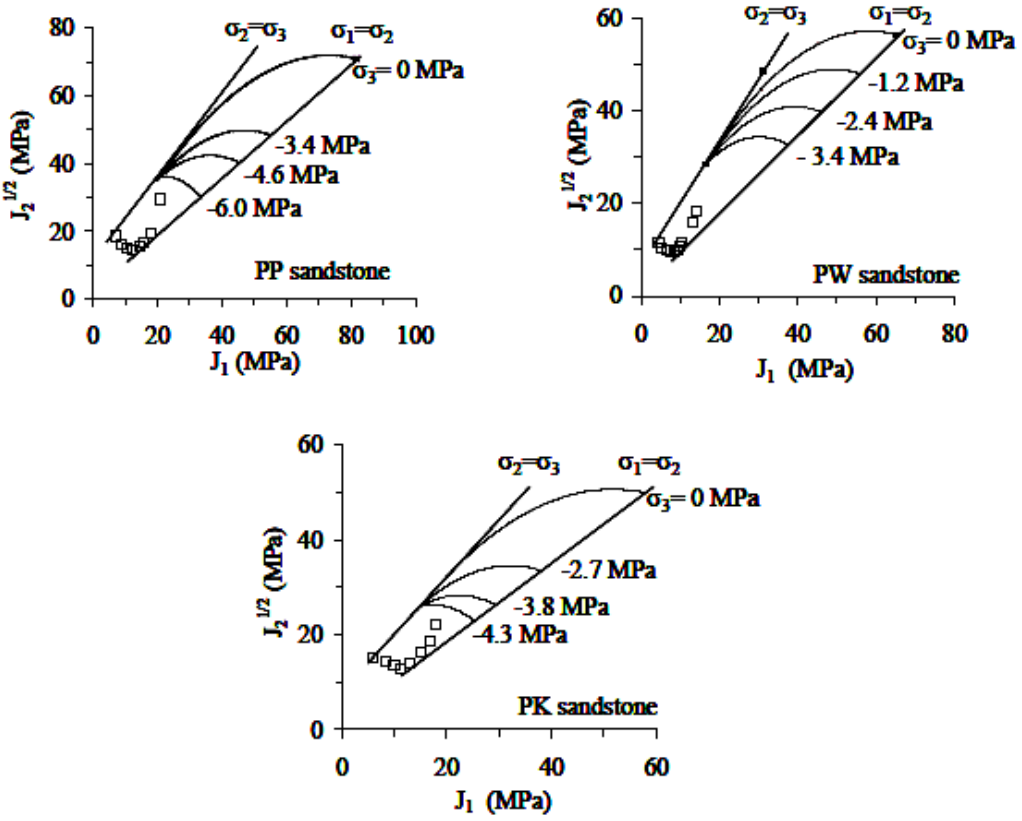

Figure 18. $J_2^{½}$ as a function of J_1 for Brazilian testing on PP, PW and PK sandstones compared with the modified Wiebols and Cook criterion.

Rock Mechanics, Fuenkajorn & Phien-wej (eds) © 2009. ISBN 978 974 533 624 7

Neoprene sheets used here can effectively reduce the friction between the rock surface and loading platen, as evidenced by the fact that σ_1 at failure measured under $\sigma_2 = \sigma_3$ for these sandstones is comparable to the corresponding triaxial compressive strengths of the rocks obtained by the conventional method (Kenkhunthod & Fuenkajorn, 2009). It can be concluded that the interface friction did not contribute to the increase of σ_1 at failure under true triaxial testing as suggested by Cai (2008).

Under true triaxial compressive stresses the modified Wiebols and Cook criterion can predict the compressive strengths of the tested sandstones reasonably well. Due to the effect of σ_2 the Coulomb criterion can not represent the rock strengths under true triaxial compressions, particularly under high σ_2 to σ_3 ratios. The Coulomb criterion however performs better when the minimum principal stress is in tension. It can describe the decrease and increase of $J_2^{1/2}$ at failure due to the variation of the minimum principal tensile stresses with the discrepancy of about 15-20%. It is clear that the modified Wiebols and Cook criterion can not be correlated with the rock strengths when the minimum principal stress is in tension

It is postulated that the effects of the intermediate principal stress are caused by two mechanisms working simultaneously but having opposite effects on the rock polyaxial strengths; (1) mechanism that strengthens the rock matrix in the direction normal to σ_1 - σ_3 plane, and (2) mechanism that induces tensile strains in the directions of σ_1 and σ_3.

The intermediate principal stress can strengthen the rock matrix on the plane normal to its direction, and hence a higher differential stress is required to induce failure. This is simply the same effect obtained when applying a confining pressure to a cylindrical specimen in the conventional triaxial compression testing. Considering this effect alone, the higher the magnitude of σ_2 applied, the higher σ_1 (or $J_2^{1/2}$) is required to fail the specimen. Nevertheless it is believed that the relationship between σ_2 magnitudes and the degrees of strengthening can be non-linear, particularly under high σ_2. Such relation depends on rock types and their texture (e.g., distribution of grain sizes, pore spaces, fissures and micro-cracks, and types of rock-forming minerals).

At the same time due to effect of the Poisson's ratio σ_2 can produce tensile strains in the directions normal to its axis (or on the plane parallel to σ_1 and σ_3). These tensile strains increase from the minimum on the mid-section plane to the maximum on the specimen surfaces where the rock can freely dilate. These tensile strains cause splitting tensile fractures of the rock specimen. This is supported by the results of the Brazilian testing under axial compression. The applied σ_z produces a tensile strains adding to the line load-induced tensile stress at the specimen center. As a result a smaller magnitude of the line load is required to split the Brazilian specimen when it is under an axial compression. Based on this mechanism alone the higher the σ_2 that is applied, the lower σ_1 or $J_2^{1/2}$ is required to fail the specimen. Since the induced tensile strains by σ_2 in the polyaxial specimen is not uniformly distributed on the σ_1 - σ_3 plane, quantitative determination of the effect of σ_2 under this mechanism is not easy. The elastic properties under tension may differ from those in compression. The calculation is also complicated by the same mechanism induced by σ_1 and σ_3. Nevertheless it is suggested that the rock polyaxial strength is governed not only by the magnitudes of the three principal stresses, but also by its deformation properties.

The two mechanisms work simultaneously during polyaxial loading but with different degrees of influence depending on the magnitudes of the principal stresses at failure and of the rock elastic properties. When σ_2 is close to σ_3 (i.e. low σ_2:σ_3 ratio or high σ_1:σ_2 ratio) the

rock is strengthened by the increase of σ_2. Under this condition, the strengthening mechanism dominates, and σ_1 at failure increases with σ_2. Here the rock fails under compressive shear mode because the tensile strain induced by σ_2 is small. The rate of rock strengthening however decreases as σ_2 increases. When σ_2 approaches σ_1 (i.e. high σ_2:σ_3 ratio or low σ_1:σ_2 ratio) the tensile strain induced by σ_2 becomes more pronounced and overcomes the strengthening rate. Under this condition, σ_1 at failure decreases with increasing σ_2, and the rock is failed by splitting tensile fractures. The different modes of failure obtained under different stress conditions have been observed from the test results here. Between the two extreme conditions above the combined effects from the two mechanisms will determine the rock polyaxial strengths and its failure characteristics. For the polyaxial strength results obtained here and elsewhere (e.g. Colmenares & Zoback, 2002; Haimson, 2006; and You, 2008) the proposed mechanisms can explain why at a given σ_3, σ_1 at failure initially increases with σ_2 when σ_2 is low, and decreases with increasing σ_2 when σ_2 becomes larger. This phenomenon is particularly obvious when σ_3 is very low. It is recommended that rock deformation properties be incorporated into a failure criterion to fully describe the rock strengths under true triaxial stresses. Deserving special attention is the derivation of a strain energy-based criterion which can take both the principal stresses and principal strains (or elastic properties) at failure into consideration.

ACKNOWLEDGTMENT

This research is funded by Suranaree University of Technology. Permission to publish this paper is gratefully acknowledged.

REFERENCES

Al-Ajmi, A.M. & Zimmerman, R.W., 2005. Relation between the Mogi and the Coulomb failure criteria. *International Journal of Rock Mechanics & Mining Sciences*. 42:431-439.

Al-Ajmi, A.M. & Zimmerman, R.W., 2005. Relation between the Mogi and the Coulomb failure criteria. *International Journal of Rock Mechanics & Mining Sciences*. 42: 431-439.

Alexeev, A.D., Revva, V.N., Alyshev, N.A. & Zhitlyonok, D.M., 2004. True triaxial loading apparatus and its application to coal outburst prediction. *International Journal of Coal Geology*. 58: 245-250.

Alexeev, A.D., Revva, V.N., Alyshevb, N.A. & Zhitlyonok, D.M., 2004. True triaxial loading apparatus and its application to coal outburst prediction. *International Journal of Coal Geology*. 58: 245-250.

ASTM D3967-95. Standard Test Method for Splitting Tensile Strength of Intact Rock Core Specimens. *Annual Book of ASTM Standards*. 04.08. American Society for Testing and Materials: Philadelphia.

ASTM D3967-95. Standard Test Method for Splitting Tensile Strength of Intact Rock Core Specimens. *Annual Book of ASTM Standards*. 04.08. American Society for Testing and Materials, Philadelphia.

ASTM D4543-85. Standard Practice for Preparing Rock Core Specimens and Determining Dimensional and Shape Tolerances. *Annual Book of ASTM Standards*. 04.08. American Society for Testing and Materials: Philadelphia.

ASTM D4543-85. Standard Practice for Preparing Rock Core Specimens and Determining Dimensional and Shape Tolerances. *Annual Book of ASTM Standards*. 04.08. American Society for Testing and Materials, Philadelphia.

Benz, T. & Schwab, R., 2008. A quantitative comparison of six rock failure criteria. *International Journal of Rock Mechanics and Mining Sciences*. 45: 1176-1186.

Rock Mechanics, Fuenkajorn & Phien-wej (eds) © 2009. ISBN 978 974 533 624 7

Cai, M., 2007. Influence of intermediate principal stress on rock fracturing and strength near excavation boundaries—Insight from numerical modeling, *International Journal of Rock Mechanics & Mining Sciences*. 45:269-772.

Cai, M., 2008. Influence of intermediate principal stress on rock fracturing and strength near excavation boundaries—Insight from numerical modeling, *International Journal of Rock Mechanics & Mining Sciences*. 45: 763-772.

Chang, C. & Haimson, B., 2005. Non-dilatants deformation and failure mechanism in two Long Valley Caldera rocks under true triaxial compression. *International Journal of Rock Mechanics & Mining Sciences*. 42: 402-414.

Chang, C. & Haimson, B., 2005. Non-dilatants deformation and failure mechanism in two Long Valley Caldera rocks under true triaxial compression. *International Journal of Rock Mechanics & Mining Sciences*. 42: 402-414.

Chen, C. H., Pan, E. & Amadei B., 1998. Determination of the deformability and tensile strength of anisotropic rocks using Brazilian tests. *International Journal of Rock Mechanics & Mining Sciences*. 35: 43-61.

Chen, C. H., Pan, E. & Amadei B., 1998. Determination of the Deformability and Tensile Strength of Anisotropic Rocks Using Brazilian tests. *International Journal of Rock Mechanics & Mining Sciences*. 35: 43-61.

Claesson, J. & Bohloli, B., 2002. Brazilian test: stress field and tensile strength of anisotropic rocks using an analytical solution. *International Journal of Rock Mechanics & Mining Sciences*.

Colmenares, L.B. & Zoback, M.D., 2002. A statistical evaluation of intact rock failure criteria constrained by polyaxial test data for five different rocks. *International Journal of Rock Mechanics & Mining Sciences*. 39: 695-729.

Colmenares, L.B. & Zoback, M.D., 2002. A statistical evaluation of intact rock failure criteria constrained by polyaxial test data for five different rocks. *International Journal of Rock Mechanics & Mining Sciences*. 39: 695-729.

Haimson, B. & Chang, C., 1999. A new true triaxial cell for testing mechanical properties of rock, and its use to determine rock strength and deformability of Westerly granite. *International Journal of Rock Mechanics and Mining Sciences*. 37: 285-296.

Haimson, B. & Chang, C., 2000. A new true triaxial cell for testing mechanical properties of rock, and its use to determine rock strength and deformability of Westerly granite. *International Journal of Rock Mechanics and Mining Sciences*. 37: 285-296.

Haimson, B., 2006. True triaxial stresses and the brittle fracture of rock. *Pure and Applied Geophysics*. 163: 1101-1113.

Haimson, B., 2006. True Triaxial Stresses and the Brittle Fracture of Rock. *Pure and Applied Geophysics*. 163: 1101-1113.

Hondros, G., 1959. The evaluation of Poisson's ratio and the modulus of materials of low tensile resistance by the Brazilian (indirect tensile) tests with particular reference to concrete. *Australian Journal of Applied Sciences*. 10: 243-268.

Hondros, G., 1959. The Evaluation of Poisson's Ratio and the Modulus of Materials of low Tensile Resistance by the Brazilian (Indirect Tensile) Tests with Particular Reference to Concrete. *Australian Journal of Applied Sciences*. 10: 243-268.

Jaeger, J.C. & Cook, N.G.W., 1979. *Fundamentals of Rock Mechanics*. London: Chapman and Hall.

Jaeger, J.C. & Cook, N.G.W., 1979. *Fundamentals of Rock Mechanics*. London: Chapman and Hall.

Jianhong, Y., Wu, F. Q. & Sun J.Z., 2008. Estimation of Tensile Elastic Modulus using Brazilian disc by applying diametrically opposed concentrated loads. *International Journal of Rock Mechanics & Mining Sciences*.

Kenkhunthod, N. & Fuenkajorn, K., 2009. Effects of loading rate on compressive strength of sandstones under confinement. *Proceedings of the Second Thailand Rock Mechanics Symposium*, Nakhon Ratchasima: Suranaree University of Technology.

Kwaśniewski, M., Takahashi, M. & Li, X., 2003. Volume changes in sandstone under true triaxial compression conditions. *ISRM 2003–Technology Roadmap for Rock Mechanics*, South African Institute of Mining and Metallurgy.

Liao, J. J., Yang, M. T. & Hsieh, H. Y. 1997. Direct tensile behavior of a transversely isotropic rock. *International Journal of Rock Mechanics & Mining Sciences*. 34(5): 831-849.

Ohokal, M., Funatol, A. & Takahashi, Y., 1997. Tensile test using hollow cylindrical specimen. *International Journal of Rock Mechanics & Mining Sciences*. Vol. 34, No. 3-4, 1997 ISSN 0148-9062.

Oku, H., Haimson, B. & Song, S.R., 2007. True triaxial strength and deformability of the siltstone overlying the Chelungpu fault (Chi-Chi earthquake), Taiwan. *Geophysical Research Letters*. 34(9).

Reddy, K.R., Saxena, S.K. & Budiman, J.S., 1992. Development of a true triaxial testing apparatus. *Geotechnical Testing Journal*. 35(2): 89-105.

Reddy, K.R., Saxena, S.K. & Budiman, J.S., 1992. Development of a True Triaxial Testing Apparatus. *Geotechnical Testing Journal*. 15(2): 89-105.

Schwab, R. & Benz, T., 2008. a quantitative comparison of six rock failure criteria. *International Journal of Rock Mechanics and Mining Sciences*. 45: 1176-1186.

Singh, B., Goel, R.K., Mehrotra, V.K., Garg, S.K. & Allu, M.R., 1998. Effect of intermediate principal stress on strength of anisotropic rock mass. *Tunneling and Underground Space Technology*. 13: 71-79.

Smart, B. G. D., 1995. A true triaxial cell for testing cylindrical rock specimens. *International Journal of Rock Mechanics and Mining Sciences*. 32(3): 269-275.

Tepnarong, P. 2001. Theoretical and Experimental Studies to Determine Compressive and Tensile Strength of Rock, Using Modified Point Load Testing. *M.S. Thesis*, Suranaree University of Technology, Thailand.

Tiwari, R.P. & Rao, K.S., 2004. Physical modeling of a rock mass under a true triaxial stress state. *International Journal of Rock Mechanics and Mining Sciences*. 41(30):2A 141-6.

Tiwari, R.P. & Rao, K.S., 2004. Physical modeling of a rock mass under a true triaxial stress state. *International Journal of Rock Mechanics and Mining Sciences*. 41(30).

Tiwari, R.P. & Rao, K.S., 2006. Post failure behaviour of a rock mass under the influence of triaxial and true triaxial confinement. *Engineering Geology*. 84: 112-129.

Wawersik, W.R., Carlson, L.W., Holcomb, D.J. & Williams, R.J., 1997. New method for true-triaxial rock testing. *International Journal of Rock Mechanics and Mining Sciences*. 34(3-4): 365-385.

Wawersik, W.R., Carlson, L.W., Holcomb, D.J. & Williams, R.J., 1997. New method for true-triaxial rock testing. *International Journal of Rock Mechanics and Mining Sciences*. 34(330): 3-4.

Wijk, G., 1978. Some new theoretical aspects of indirect measurements of tensile strength of rock. *International Journal of Rock Mechanics & Mining Sciences*. 15: 149-160.

Yang, X. L., Zou, J. F. & SUI, Z. R., 2007. Effect of intermediate principal stress on rock cavity stability. *Journal Central South University Technology*. s1-0165-05

You, M., 2008. True-triaxial strength criteria for rock. *International Journal of Rock Mechanics and Mining Sciences*. 46: 115-127.

You, M., 2008. True-triaxial strength criteria for rock. *International Journal of Rock Mechanics and Mining Sciences*. 46: 115-127.

Effects of Intermediate Principal Stress on Compressive and Tensile Strengths of Sandstones

Paper No.298

R. Thosuwan **C. Walsri** **P. Poonprakon** **K. Fuenkajorn**
Suranaree University of technology
Nakorn Ratchasima

ABSTRACT

A series of true triaxial compression tests and indirect tension tests with axial confinements are performed to assess the effects of the intermediate principal stresses on the elasticity and strengths of three types of sandstones. These sandstones are commonly found in the north and northeast of Thailand. Their mechanical properties and responses play a significant role on the stability of the tunnels, slope embankments and dam foundations in the region. A true understanding of the failure behavior of these rocks is highly desirable. In particular, knowledge of the rock tensile strength as affected by the intermediate principal stress is rare.

Over 50 rectangular shaped specimens (50x50x100 mm) are tested using a polyaxial load frame. Lateral stresses are applied with different magnitudes between two mutually perpendicular directions ($\sigma_2 \neq \sigma_3$), and varying from 0 up to 20 MPa. The axial stress (σ_1 - along the longest axis) is increased until failure. Neoprene caps are inserted at the interfaces between loading platens and specimen surfaces to minimize the friction. The failure stresses are presented in form of octahedral shear strength (τ_{oct}) vs. mean stress (σ_m) diagram. Comparisons of the results with those obtained from the uniaxial and triaxial strength testing indicate that under the same σ_m, σ_2 can notably decrease the τ_{oct} at failure. The failure envelope is lower for the greater σ_2/σ_3 ratio. The results also indicate that the sandstones are transversely anisotropic. The elastic modulus in the direction normal to the bedding planes is about 2-4 times greater than that parallel to the bedding planes. The Poisson's ratio on the plane parallel to the beds is about three times smaller than that across the beds. These hold true for all sandstones tested here.

The effect of σ_2 on the tensile strengths is assessed by conducting the indirect tension test under confinement. The constant σ_2 with magnitudes varying from 0 to 40 MPa is applied along the axial direction of 50 mm-diameter disk samples using the polyaxial load frame. Then the line load is diametrically applied until failure occurs. The intermediate principal stress (σ_2 - axial stress in this case) significantly decreases the magnitude of the line load required to fail the disk samples. Using linear elastic theory the stress states are derived for the sample center (where the tensile crack is initiated) which is under uniaxial strain condition. A more complete failure criterion (taken σ_2 into consideration) is developed using τ_{oct} - σ_m diagram by combining the results of tension test under confinements with those of the true triaxial compression tests. The octahedral shear strengths of the rocks under the mean stresses that are lower than that obtained from the uniaxial compressive strength can be obtained.

Key Words: sandstone, true triaxial, polyaxial, intermediate principal stress, Brazilian test

BIOGRAPHY

Mr. Chaowarin Walsri was born on December 6, 1983 in Samut songkhram province, Thailand. He received his Bachelor's Degree in Engineering (Geotechnology) from Suranaree University of Technology in 2006. For his post-graduate, he continued to study with a Master's degree in the Geological Engineering Program, Institute of Engineering, Suranaree university of Technology. During graduation, 2007-2009, he was a part time worker in position of research assistant at the Geomechanics Research Unit, Institute of Engineering, Suranaree University of Technology. He has published two technical papers related to rock mechanics, titled Compressive and Tensile Strengths of Sandstones under True Triaxial Stresses published in the Proceeding of the Second Thailand symposium on rock mechanics, Chonburi, Thailand; and Effects of Intermediate Principal on Compressive and Tensile Strengths of Sandstones in the Proceeding of International Symposium on Rock Mechanics, University of Hong Kong, Hong Kong. For his work, he is a good knowledge in geomechanics theory and practice.